Astronuclear Laboratory

WANL-PR(XXX)-001

MODIFICATION AND CONTROL OF OXIDE STRUCTURES ON METALS AND ALLOYS

FINAL REPORT
(20 November 1969 to 20 November 1970)
April 1971

by

R. C. Svedberg

Prepared Under Contract N00019-70-C-0148

for

NAVAL AIR SYSTEMS COMMAND
Department of the Navy
Washington, D. C. 20360
Attn: I. Machlin
Air 52031B

by

WESTINGHOUSE ASTRONUCLEAR LABORATORY
WESTINGHOUSE ELECTRIC CORPORATION
P. O. BOX 10864
PITTSBURGH, PENNSYLVANIA 15236

86

Security Classification

DOCUMENT CONTROL DATA - R&D

(Security classification of title, body of abstract and indexing annotation must be entered when the overall report is classified)

1. ORIGINATING ACTIVITY (Corporate author) Westinghouse Astronuclear Laboratory P. O. Box 10864 Pittsburgh, Pa. 15236	2a. REPORT SECURITY CLASSIFICATION Unclassified 2b. GROUP N/A

3. REPORT TITLE

Modification and Control of Oxide Structures on Metals and Alloys

4. DESCRIPTIVE NOTES (Type of report and inclusive dates)

Final Technical Report - 20 November 1969 to 20 November 1970

5. AUTHOR(S) (Last name, first name, initial)

Svedberg, Robert C.

6. REPORT DATE	7a. TOTAL NO. OF PAGES	7b. NO. OF REFS

8a. CONTRACT OR GRANT NO.	9a. ORIGINATOR'S REPORT NUMBER(S)
N00019-70-C-0148 b. PROJECT NO. c. APPROVED FOR PUBLIC RELEASE; DISTRIBUTION UNLIMITED d.	WANL-PR(XXX)-001 9b. OTHER REPORT NO(S) (Any other numbers that may be assigned this report)

10. AVAILABILITY/LIMITATION NOTICES

This document is subject to special export controls and each transmittal to foreign governments or foreign nationals may be made only with the approval of the Naval Air Systems Command.

11. SUPPLEMENTARY NOTES	12. SPONSORING MILITARY ACTIVITY
Details of illustrations in this document may be better studied on microfiche	Naval Air Systems Command Washington, D. C. 20360

13. ABSTRACT

The feasibility of modifying oxide defect structures to enhance oxidation protection of elevated temperature structural materials was investigated. High-pressure, high-temperature techniques and pre-oxidation treatments were used to modify the oxide structure.

Nb_2O_5 when subjected to high pressures (78 kbar) and high temperatures transformed to a denser structure with a density increase of about 25%.

Nb, Ta, and the niobium alloy, B-1 (Nb-15Ti-10Ta-10W-2Hf-2.5Al) were pretreated in an autoclave containing Fe^{3+} ions and a mixed oxide, rutile type tapiolite structure was formed. These films decreased the initial oxidation rate of pure niobium in 20 torr oxygen at 650°C. However, the films caused an increased oxidation rate for pure niobium and tantalum in air at 1060°C when compared to the untreated metals.

The oxidation behavior of the B-1 niobium alloy at 1060°C in air was enhanced by a 3-4 hour pre-exposure in 20 torr oxygen at 650°C. Metallographic and x-ray analyses indicated that less TiO_2 was formed in the oxide film grown on these samples.

In addition, many techniques reported in the literature for altering the oxidation behavior of various metal and alloy systems were reviewed.

DD FORM 1 JAN 64 1473

UNCLASSIFIED

Security Classification

Security Classification

14 KEY WORDS	LINK A		LINK B		LINK C	
	ROLE	WT	ROLE	WT	ROLE	WT
Oxide Defect Structure Oxidation Protection High Pressure Pretreatments						

INSTRUCTIONS

1. ORIGINATING ACTIVITY: Enter the name and address of the contractor, subcontractor, grantee, Department of Defense activity or other organization *(corporate author)* issuing the report.

2a. REPORT SECURITY CLASSIFICATION: Enter the overall security classification of the report. Indicate whether "Restricted Data" is included. Marking is to be in accordance with appropriate security regulations.

2b. GROUP: Automatic downgrading is specified in DoD Directive 5200.10 and Armed Forces Industrial Manual. Enter the group number. Also, when applicable, show that optional markings have been used for Group 3 and Group 4 as authorized.

3. REPORT TITLE: Enter the complete report title in all capital letters. Titles in all cases should be unclassified. If a meaningful title cannot be selected without classification, show title classification in all capitals in parenthesis immediately following the title.

4. DESCRIPTIVE NOTES: If appropriate, enter the type of report, e.g., interim, progress, summary, annual, or final. Give the inclusive dates when a specific reporting period is covered.

5. AUTHOR(S): Enter the name(s) of author(s) as shown on or in the report. Enter last name, first name, middle initial. If military, show rank and branch of service. The name of the principal author is an absolute minimum requirement.

6. REPORT DATE: Enter the date of the report as day, month, year; or month, year. If more than one date appears on the report, use date of publication.

7a. TOTAL NUMBER OF PAGES: The total page count should follow normal pagination procedures, i.e., enter the number of pages containing information.

7b. NUMBER OF REFERENCES: Enter the total number of references cited in the report.

8a. CONTRACT OR GRANT NUMBER: If appropriate, enter the applicable number of the contract or grant under which the report was written.

8b, 8c, & 8d. PROJECT NUMBER: Enter the appropriate military department identification, such as project number, subproject number, system numbers, task number, etc.

9a. ORIGINATOR'S REPORT NUMBER(S): Enter the official report number by which the document will be identified and controlled by the originating activity. This number must be unique to this report.

9b. OTHER REPORT NUMBER(S): If the report has been assigned any other report numbers *(either by the originator or by the sponsor)*, also enter this number(s).

10. AVAILABILITY/LIMITATION NOTICES: Enter any limitations on further dissemination of the report, other than those imposed by security classification, using standard statements such as:

(1) "Qualified requesters may obtain copies of this report from DDC."

(2) "Foreign announcement and dissemination of this report by DDC is not authorized."

(3) "U. S. Government agencies may obtain copies of this report directly from DDC. Other qualified DDC users shall request through _____."

(4) "U. S. military agencies may obtain copies of this report directly from DDC. Other qualified users shall request through _____."

(5) "All distribution of this report is controlled. Qualified DDC users shall request through _____."

If the report has been furnished to the Office of Technical Services, Department of Commerce, for sale to the public, indicate this fact and enter the price, if known.

11. SUPPLEMENTARY NOTES: Use for additional explanatory notes.

12. SPONSORING MILITARY ACTIVITY: Enter the name of the departmental project office or laboratory sponsoring *(paying for)* the research and development. Include address.

13. ABSTRACT: Enter an abstract giving a brief and factual summary of the document indicative of the report, even though it may also appear elsewhere in the body of the technical report. If additional space is required, a continuation sheet shall be attached.

It is highly desirable that the abstract of classified reports be unclassified. Each paragraph of the abstract shall end with an indication of the military security classification of the information in the paragraph, represented as *(TS), (S), (C), or (U)*.

There is no limitation on the length of the abstract. However, the suggested length is from 150 to 225 words.

14. KEY WORDS: Key words are technically meaningful terms or short phrases that characterize a report and may be used as index entries for cataloging the report. Key words must be selected so that no security classification is required. Identifiers, such as equipment model designation, trade name, military project code name, geographic location, may be used as key words but will be followed by an indication of technical context. The assignment of links, rules, and weights is optional.

UNCLASSIFIED

Security Classification

Astronuclear Laboratory

WANL-PR(XXX)-001

MODIFICATION AND CONTROL OF OXIDE STRUCTURES ON METALS AND ALLOYS

FINAL REPORT
(20 November 1969 to 20 November 1970)
April 1971

Details of illustrations in this document may be better studied on microfiche

by

R. C. Svedberg

Prepared Under Contract N00019-70-C-0148

for

NAVAL AIR SYSTEMS COMMAND
Department of the Navy
Washington, D. C. 20360
Attn: I. Machlin
Air 52031B

by

WESTINGHOUSE ASTRONUCLEAR LABORATORY
WESTINGHOUSE ELECTRIC CORPORATION
P. O. BOX 10864
PITTSBURGH, PENNSYLVANIA 15236

BLANK PAGE

FOREWORD

The work described herein was done at the Astronuclear Laboratory of the Westinghouse Electric Corporation under Navy Contract N00019-70-C-0148. I. Machlin of the Naval Air Systems Command served as Project Monitor. Program supervision at WANL was by Mr. R. W. Buckman, Jr., Manager, Materials Science.

The author wishes to acknowledge additional personnel contributing to this program. These are: Mr. W. Hess for oxidation testing, Mr. K. J. Galbraith for metallography, Messrs R. W. Conlin and A. W. Danko for x-ray diffraction, and Dr. A. Taylor and N. J. Doyle of the Westinghouse Research and Development Center for the high pressure experiments.

MODIFICATION AND CONTROL OF OXIDE STRUCTURES ON METALS AND ALLOYS

ABSTRACT

The feasibility of modifying oxide defect structures to enhance oxidation protection of elevated temperature structural materials was investigated. High-pressure, high-temperature techniques and pre-oxidation treatments were used to modify the oxide structure.

Nb_2O_5 when subjected to high pressures (78 kbar) and high temperatures transformed to a denser structure with a density increase of about 25%.

Nb, Ta, and the niobium alloy, B-1 (Nb-15Ti-10Ta-10W-2Hf-2.5Al) were pretreated in an autoclave containing Fe^{3+} ions and a mixed oxide, rutile type tapiolite structure was formed. These films decreased the initial oxidation rate of pure niobium in 20 torr oxygen at 650°C. However, the films caused an increased oxidation rate for pure niobium and tantalum in air at 1060°C when compared to the untreated metals.

The oxidation behavior of the B-1 niobium alloy at 1060°C in air was enhanced by a 3-4 hour pre-exposure in 20 torr oxygen at 650°C. Metallographic and x-ray analyses indicated that less TiO_2 was formed in the oxide film grown on these samples.

In addition, many techniques reported in the literature for altering the oxidation behavior of various metal and alloy systems were reviewed.

TABLE OF CONTENTS

TABLE OF CONTENTS (CONTINUED)

LIST OF TABLES

LIST OF FIGURES

I. INTRODUCTION AND SUMMARY

This study was initiated to investigate the feasibility of modifying oxide defect structures to enhance oxidation protection of elevated temperature structural materials. Materials capable of performing at temperatures in excess of 2000°F in oxidizing environments without degradation are being demanded for use in air breathing propulsion engines and power generation systems. The great majority of the research effort to provide materials capable of fulfilling the requirements of structural integrity at elevated temperatures and in oxidizing environments have involved attempts to increase oxidation resistance by adding additional alloying elements to the basic structural material or by coating the basic structural alloy with an oxidation resistant material. However, alloying to obtain oxidation resistance, in most cases, alters the mechanical strength and ductility of the base structural material while coating to obtain oxidation resistance requires the application of a foreign refractory compound which must adhere to, but not react, with the structural substrate. In addition, coatings are also subject to damage by thermal shock and physical impact.

The approach for providing oxidation protection being investigated in this program is considered rather unique in light of the prior research and development programs reported in the literature. Techniques are being investigated which are designed to modify the defect structure of equilibrium oxides which are characteristic of the parent structural material. In this way an improvement in oxidation resistance can be realized without changing the structural and mechanical properties of the substrate or adding additional phases or compounds to the system. Modifying the parent oxide to decrease the transport of anions and cations through the lattice, or to improve the adherence between the oxide and the substrate by stabilizing a denser oxide phase will improve the oxidation resistance.

This program involved (1) testing several techniques for modifying oxide defect structures, and (2) reviewing the literature for (a) other techniques which have been successful in improving the oxidation resistance of high temperature materials, (b) methods to modify the defect structure of oxides, and (c) information which would lead to the formulation of original new

ideas to prevent oxidation and structural deterioration in oxygen environments at elevated temperatures. Of the many techniques reported to modify oxide characteristics such as adding ions of different valence, applying electric fields, and thermal treatments, two techniques emerged as being unexplored, but holding special promise. These techniques are (1) high pressure–high temperature exposures of oxides and (2) pretreatments of the metals and alloys prior to service exposure. These basic techniques have been tried with some degree of success during this program, each being designed to stabilize an adherent oxide structure with transport kinetics which are slower than those of the non-protective oxide which forms under service exposure.

The need for an oxidation resistant refractory metal component for use in air breathing engines led to the selection of Nb_2O_5* as the material for investigation in the high pressure study. Also, Cb, Ta, and an oxidation resistant niobium alloy B-1 (Nb-15Ti-10Ta-10W-2Hf-2.5Al) were selected as material upon which to investigate the effect of autoclave exposure and low pressure oxygen pretreatment on the oxide formed and hence, the oxidation behavior.

The goal of the high temperature–high pressure exposure was to produce phases with a denser structure or to decrease the concentration of vacancies in the oxide structure and thereby decrease transport rates. The pre-oxidation treatment in 20 mm oxygen pressure at 650°C was designed to form or nucleate a stable oxide which would either inhibit transport of oxygen to the metal or would serve as nuclei to encourage the growth of a protective phase. The autoclave exposure at 350°C was designed to stabilize the dense low temperature oxide phase by the addition of Fe^{3+} to the parent oxide of the structural materials. The portion of the program devoted to reviewing the literature, however, was not limited to the metal and alloy systems investigated, but involved the study of all the refractory metals and alloys and the nickel-cobalt based alloys known as superalloys. The literature pertaining to novel techniques used to achieve some degree of improved oxidation protection was closely

* Nb is also called columbium (Cb).

examined. No attempt was made to compile and sort the vast quantities of oxidation data. For this information the readers are referred to the works of Kofstad[1], Hauffe[2], and Kubaschewski and Hopkins[3].

The results of the experimental program can be summarized briefly. Pretreatment of the niobium alloy B-1* at 660°C and in 2.6×10^{-2} atmospheres (20 torr) oxygen pressure significantly reduced the oxidation rate during subsequent exposure in one atmosphere of air at 1060°C. The pretreated alloy B-1 exhibited an oxidation rate of about 25% less than untreated material. The improved oxidation behavior appears to be due to the formation of less TiO_2 in the scale as a result of the 20 torr pre-exposure. The pretreatment of pure niobium and tantalum in 20 torr oxygen resulted in sufficient oxidation to preclude further exposure in air. It appears that the pre-exposure technique can be more easily applied to the alloys, where the conditions of treatment can affect the rate of formation of more complex and protective oxides. The films grown during the autoclave exposures affected the rate curve for the oxidation of pure Nb in 20 torr oxygen which showed initially slower oxidation. However, only one autoclave pretreatment environment could be evaluated within the scope of the program.

The combined effects of temperature and pressure produced significant changes in the crystal structure of Nb_2O_5. By heating at 1200°C and applying a pressure of 56 and 78 kbar αNb_2O_5** was converted to $\gamma + \gamma'$ Nb_2O_5** which is stable at room temperature. Most significantly, the density has increased from 4.56 to 5.81 gm/cm^3. Such an increase in density suggests significant alteration in transport properties and hence oxidation behavior. The high density form of the Nb_2O_5 was reconverted to α-Nb_2O_5 after heating for one hour at 1000°C in air. Future experimentation is necessary to more adequately define the P-T diagram of Nb_2O_5. Also study must be considered in the area of cation substitution to promote stabilization of the high pressure modifications.

---

* Nb-15Ti-10W-10Ta-2Hf-2.5Al

** Notation based on Terao[4] and Brauer[5].

Pretreatments show promise of being able to selectively form protective scales on the surface of an alloy. This has been demonstrated in this program for the B-1 niobium alloy, but the principles and treatments involved can be adapted to other alloys. Work is needed to understand the mechanisms responsible for this enhancement in oxidation protection so that pretreatment processes can be designed for a given alloy. Although little effect was found as a result of the autoclave pre-exposure, the feasibility of forming films on the surface of materials by this technique has been demonstrated.

High pressure techniques are able to change the structure of oxides. For Nb_2O_5 studied in this program, an increase in the density of the structure was achieved. Questions concerning the stability of the high pressure oxides remain to be answered as do questions concerning the effect of binary oxide additions on stabilizing the protective structures produced by the high pressure treatment.

Now that it has been demonstrated thar pre-oxidation does have an effect on oxidation rates, the potential magnitude of this effect should be determined for refractory metal alloys. This involves understanding the factors which affect the oxidation behavior, such as the reaction rates of individual alloying elements under pre-oxidation conditions, the transport properties of the participating species, i.e., alloying elements and oxygen in the metal and cations, anions and electrons in the scale.

The use of autoclave techniques and high pressure techniques could then be used to facilitate the formation of protective scales.

II. REVIEW OF THE LITERATURE

Only the literature concerned with various techniques which cause improved oxidation behavior or show potential for causing improved oxidation behavior are reported. The various techniques used were categorized as (1) Pre-oxidation, (2) Effects of Foreign Ion Additions, (3) Heat Treatment of Scales, (4) Oxidizing Substrate Thickness, (5) Electric Fields, and (6) High Pressure Modification of Oxide Structures.

2.1 Pre-Oxidation

Pre-oxidation of structural materials under the proper conditions may incubate a stable oxide structure whose protective growth can be sustained at higher temperatures. The improvement in protective behavior by pretreatment has been experimentally demonstrated.[6,7] In one experiment, two identical niobium alloy specimens (Nb-15Ti-10W-10Ta-2Hf-3Al) were oxidized at 2000°F. One specimen was pre-exposed one (1) hour at 2400°F in air, prior to oxidation testing at 2000°F. As shown in Figure 1, the oxidation rate of the pre-exposed sample was significantly lower than that of the specimen given no prior treatment. Note that in Figure 1, the apparent parabolic rate constant is plotted as a function of time, hence the changes shown are quite significant. The changes in oxidation rate achieved by this pre-oxidation were greater than those obtained by a large number of compositional modifications of the basic niobium alloy.[6] The reasons for this increased protection are not fully understood and are still under consideration.

In another experiment the nitridation resistance of a Cr-0.22Y alloy was significantly improved by a low oxygen partial pressure pre-oxidation treatment.[7] A black, tightly adherent oxide film was formed on specimens exposed in a hydrogen atmosphere furnace (dew point approximately -40°F) for two (2) hours at 1500°F. The pre-oxidation treatment resulted in a significant alteration of the nitridation behavior of the Cr-0.22Y alloy as shown by the data in Table 1 which is also graphically presented in Figure 2. These limited data indicate that an oxide scale formed by the low pressure oxygen pretreatment provided an effective barrier to nitrogen diffusion.

2.2 Effects of Foreign Ion Additions

Lithiding chromium by electro-depositing a Cr-Li layer on the surface has been shown to (1) reduce the oxidation rate, (2) improve resistance to spalling, and (3) increase resistance to nitride formation during air oxidation. Tedmon and Hagel[8] have attributed this decrease in oxidation rate to a Verwey-Hauffe mechanism where Li^{+1} ions substitute for Cr^{3+} ions in the cation sublattice, thereby reducing the Cr^{3+} vacancy concentration. Since it is reasonably well established that cation diffusion controls oxidation rates of alloys which form Cr_2O_3 protective scales, decreasing the cation vacancy concentration results in slower cation diffusion rates and therefore slower oxidation rates. This oxidation resistance of lithided chromium has been tested in the temperature range from 1100°-1300°C. Attempts to oxidize the samples at high temperatures resulted in rapid volatilization of lithium from the coating.

Bhat and Khan[9] have reported that the oxidation of Ta, Nb, and W powders and sheet samples in pure oxygen can be reduced by mixing or coating the material with a 5% KHF_2 (potassium bifloride) solution. Geschwind[10] showed this same behavior when the refractory metal powders are mixed with Li_2O. Both of these materials, KHF_2 and Li_2O, are termed "negative catalysts" by the authors in that they decrease the oxidation rate in oxygen. In the case of the oxidation of the sheet material at constant temperature the oxidation rate is decreased, whereas the temperature at which the powders catastrophically oxidize on heating is raised when compared to the untreated material. Geschwind[10] attributes the enhancement in oxidation resistance to a reaction of the metal with the OH ion chemisorbed on the metallic surface; the OH radical being formed via a reaction involving Li_2O at 450°C. This chemisorption of OH ions on the metallic surface reduces the probability of chemisorption of the oxygen onto the surface which is the initial step of the oxidation process.

By adding Fe^{3+} ions to a TaO_2 oxide via an autoclave exposure of Ta to water at 300°F, a structure (Ta, Fe/O_2) was formed that resisted transformation to α-Ta_2O_5 after exposure to air at 1000°C for 10 minutes.[11] This is contrasted to a TaO_2 film without Fe^{3+} in the

lattice which did transform to α-Ta_2O_5 after the same exposure. This effect was attributed to the phase stabilization resulting from doping the TaO_2 rutile lattice structure with Fe^{3+} ions.

The feasibility of utilizing this approach to form a stable film on refractory metals is being evaluated in this program. The ability of Fe^{3+} ions to stabilize a TaO_2 structure also has intriguing possibilities. The formation of a (Ta,Fe) O_2 oxide or a (Nb, Fe) O_2 are both equally feasible. (Ta,Fe) O_2 is a naturally occurring mineral called tapiolite while (Nb,Fe) O_2 is a mineral called columbite or mossite. These minerals are not entirely pure in the naturally occurring forms. However, the controlled laboratory synthesis of these compounds is possible, as described in Reference 11. Other than the crystal structure determination, additional study of the properties of these materials has not been found. The phase relations, melting points, densities, and other properties of these materials are not known.

Goldschmidt[12] has formed binary oxide systems of Nb_2O_5 with the oxides NiO, Co_3O_4, Fe_2O_3, Cr_2O_3, V_2O_5, TiO_2, ZrO_2, WO_3, Ta_2O_5, SrO, MgO, CaO, BiO, CeO and Al_2O_3 and surveyed the phase relationships as cooled from the liquid state and after equilibration at 800°C. Some tentative binary phase fields have been established. This work has shown that these oxide additions stabilize the rutile and columbite structures. This fact substantiates the effect of the Fe^{3+} ions in the autoclave exposure stabilizing the rutile structure of the (Fe, Ta) O_2 mixture. The metal ions which stabilize the rutile structure are Ni, Co, Fe, Cr, V and Ti. Cu and Zr tend to stabilize the columite structure. Cr_2O_3 and ZrO_2 each form a single phase, $CrNbO_4$ and stabilized cubic ZrO_2 without a transformation from columbite to rutile as temperature increases. Spretnak and Speiser[13] have investigated the use of niobates as self-regenerative protective coatings for niobium based alloys. They have reported the melting temperature of some of the niobates. This information plus the information of Goldschmidt's phase relationships gives an indication of the stability and upper temperature limit of these niobates.

2.3 Heat Treatment of Scales

The third area of major interest, that of heat treatment of an equilibrium oxide under non-standard conditions, has many interesting possibilities. The following pretreatments have demonstrated some degree of success in either reducing oxidation rates or stabilizing an oxide structure. A Co-10w/oCr alloy was oxidized, subjected to a vacuum annealing treatment, and then re-oxidized.[14] The oxidation rate after vacuum anneal was lower than that observed before the vacuum annealing treatment. The reduction in oxidation rate is attributed to a physical reduction in the area for diffusion in CoO lattice by the $CoCr_2O_4$ spinel phase formed during vacuum anneal. This improvement in oxidation behavior at 900°C is dependent on the duration of the vacuum annealing treatment. However, the improvement after 36 hours of vacuum annealing was insignificant. At 900°C and up to 26 hours oxidation after vacuum annealing, the oxidation appeared to remain parabolic. However, the oxidation rate at 1100°C, after a 25 hour vacuum anneal, began to accelerate to the pre-annealed rate after about 12 to 16 hours, indicating a redistribution of the protective barrier formed during vacuum annealing.

Work currently in progress at Westinghouse Research and Development Center has demonstrated the effect of aging treatments on improving the corrosion resistance of Zr-2.5% Nb alloys in high pressure water and steam.[15] Although the exact reason for this behavior is not yet fully understood, it has been determined that aging at 500°C or 600°C forms micron sized needle-like particles in the Zr-Nb structure. The improved oxidation is directly related to the amount of precipitate formed and hence, aging time and temperature. However, whether the enhanced corrosion resistance is the result of composition changes due to precipitation or to growth characteristics of the oxide film which have resulted from some surface phenomena effected during the aging is currently the object of investigation.

2.4 Oxidizing Substrate Thickness

Mendel and Pollack[16] have determined that the thickness of a film of metal determines the extent of oxidation of the film. They have attributed this to the establishment of an equili-

brium between the vacancies created in the film as the result of the cations being removed from the film and being transported through the oxide. When the energetics are considered, the degree of oxidation is controlled or regulated by the differences in the energy required to create a larger than equilibrium concentration of vacancies in the film relative to the driving force for transport and combination of the cations with the oxygen. This model is limited to cation diffusion controlled, strongly adherent oxide films. Gibbs[17] has also investigated this vacancy control of oxidation kinetics. It is theoretically possible to form a thin film of metal on a thin layer of adherent oxide and to control oxidation using the vacancy controlled oxide thickness.

2.5 Electrical Fields

Most of the oxides formed during high temperature oxidation are ionic in nature. Thus, by applying an electric field across the side, one should be able to increase or decrease the oxidation rates by changing the polarity of the field. Uhlig and Brenner,[18] Cismaru and Cismaru,[19] and Lawless and Lombard[20] attempted to influence the oxidation rate of metals by applying a field between the sample and an electrode situated in the gaseous environment. Apparently the greatest potential drop occurred across the gas phase while the potential drop across the oxide was insufficient to affect the oxidation rates. Subsequently, Schein, LeBoucher, and Lacombe[21] and Jorgensen[22,23] have demonstrated that the electric field, when applied between the gas–oxide interface and the metal substrate does affect the oxidation rate. This has been demonstrated for iron, silicon and zinc. Zaplatynsky[24] has demonstrated, by a determination of the electrical potential across the oxide scale of Ta, Nb, and Mg during oxidation, that the polarity of the measured potential is opposed to that postulated in the various theoretical treatments proposed for oxidation processes. The metal electrode is negative with respect to the oxide electrode. Zaplatynsky has shown that the magnitude of the potential does not depend on oxide thickness and that the polarity of the measured potential has a retarding effect on oxidation. By shorting the oxide electrode with the metal electrode, the oxidation rate was increased.

Berkowitz-Mattuck[25] has shown that by immersing nichrome electrodes in an oxidizing flame (ionized plasma) and applying a potential to the electrodes, the anode (positive electrode) was observed to corrode far less than the cathode, both in sulfur bearing and non-sulfur bearing flames. This lends itself to the possible use of a sacrificial electrode in a turbine engine flame environment to protect the turbine blade material.

2.6 High Pressure Modification of Oxide Structures

There are three basic kinds of modifications that can be obtained by employing high pressure, elevated temperature techniques:

- Formation of new phases due to a shift in the equilibrium characteristics of the system.
- Synthesization of compounds which are metastable or unstable at one atmosphere.
- Compaction of oxide structures to eliminate defects such as microcracks or vacancies.

Some of the limitations and ramifications of each of these items will be described below.

2.6.1 Formation of New Phases

Kaufman[26,27] presents an analysis of the thermodynamic factors which control the effects of pressure on the phase transformations of materials. One must consider the relationship between phase equilibrium and the free energy of a given system to evaluate the effect of pressure on the interaction between the phase equilibrium (relationship between the composition and temperature), the crystal structure of the system and the thermodynamic properties such as entropy and enthalpy of formation.

If one describes the free energy of a phase i of component A at a given temperature and pressure by:

$$F_A^{\,i}(T,P) = F_A^{\,i}(T) + \int_{Po}^{P} V_A^{\,i}\, dP \quad \text{(cals/mole)} \qquad (1)$$

where $F_A^{\,i}$ (T) is the free energy at atmospheric pressure, and Po = 1 atmosphere, then for a crystal structure change $\alpha \rightarrow \beta$, the expression for the free energy change can be described as

$$\Delta F_A^{\alpha \rightarrow \beta} (T,P) = \Delta F_A^{\alpha \rightarrow \beta} (T) + \int_{Po}^{P} \Delta V_A^{\alpha \rightarrow \beta} \, dP \qquad (2)$$

By differentiating equation (2) one obtains the Clausius-Clapeyron equation

$$\left(\frac{dT}{dP}\right)_{T_A^{\alpha}}^{\alpha \rightarrow \beta} = \left(\frac{\Delta V}{\Delta S}\right)_{T_A^{\alpha}}^{\alpha \rightarrow \beta} = T_A^{\alpha} \left(\frac{\Delta V}{\Delta H}\right)_{T_A^{\alpha}}^{\alpha \rightarrow \beta} \qquad (3)$$

where T_A^{α} is the $\alpha \rightarrow \beta$ transition temperature. Thus, by knowing the sign of $\Delta V^{\alpha \rightarrow \beta}$, which can be estimated by crystallographic structure information, $\Delta S^{\alpha \rightarrow \beta}$ or $\Delta H^{\alpha \rightarrow \beta}$, the probability of achieving a change in the transformation temperature with pressures can be determined.

The value of $\frac{dT}{dP}$ can be either negative or positive,[28] while the pressure induced transformations require a negative volume change or densification of a material. This means that either a positive or negative entropy change is possible for a pressure induced transformation.

The shift in phase equilibrium can mean in the case of multi-component systems not only a change in transformation temperature, but also a shift in the compositions ct which phase boundaries are determined and changes in the mutual solubility relationship in a system.

Rooymans[28] presents a paper which describes the general characteristics of high pressure chalcogenide structures. The difficulty of determining a priori which crystal structure will be in equilibrium at high pressure is explained by Rooymans.

In general, pressure applied to a structure will tend to increase its coordination number (pressure coordination rule).[29] However, this can be used as a general rule only if one assumes the radius of the spheres atoms comprising the compound is constant and independent of structure, and that the compressibility of spheres is independent of the coordination number.

Goldschmidt[30] has given evidence that a decrease in coordination number is accompanied by a decrease in interatomic distance.

The effect of compression on the coordination number must also be considered. In general the compressibility of an atom will be larger for a smaller coordination number. Depending on the compressibilities of the element and coordination number, it is quite possible for a fcc structure to transform to a bcc structure under pressure. For instance the density of a bcc structure and a fcc structure can be the same if the radius of the atoms are only 3% less in the bcc structure than in a fcc structure. Thus the conception that pressure will produce a closer packed structure, i.e., one with a larger coordination number, is not always true. This behavior is exhibited for strontium.[31] In oxide lattices, the difference in compressibilities between the cation and the anion gives additional deviations from the pressure coordination rule. In general the large anions will shrink more under compression than the cations. This will enable the cations to accommodate more anions around them, thereby increasing the coordination number for the cations.

Rooymans makes the general statement that for the chalcogenides reviewed in his paper,[28] the occurrence of a really novel structure is exceptional. The structure generally adopted for an element under high pressure conditions is in many cases the structure found for a heavier element from the same group in the periodic system. Even in the case of compounds, the high pressure modifications have the structure expected for a compound with a larger value of the cation/anion radius ratio. Coesite, a high pressure modification of SiO_2 was the first novel structure to be synthesized as a high pressure compound.[32] Indeed novel structures are quite exceptional.

Table 2 presents a list of many of the oxide compounds of high temperature structural materials which have been studied at elevated pressures. Included in the table are the structures involved in the transformation and the pressure and temperature conditions at which the phenomena occur. For many of the oxides listed, no phase change was noted.

In this case, the pressures and temperatures indicated are the extremes below which no transformation took place.

ZrO_2 transformed to its high temperature monoclinic phase at room temperature, the percentage transformation being a function of the pressure above the equilibrium transformation pressure as described by the P-T phase diagram for ZrO_2.[33]

The transition metal monoxides, FeO, CoO, NiO and MnO did not exhibit a phase change up to 265 kbar pressure at room temperature. The rutile structure was always formed after high pressure exposure for TiO_2, whether one started with the rutile phase or anatase phase. The oxides A_2X_3, including α-Al_2O_3, Cr_2O_3, and α-Fe_2O_3 did not undergo phase transformations as the result of high pressure exposure.[28]

No work was found which described the Nb_2O_5 and Ta_2O_5 behavior at elevated pressures. TiO, VO, and NbO[34] have been exposed to $\approx$90,000 kbar-°C with no resultant phase transformation. These compounds will be discussed later in this report.

Table 3 shows a compilation of the various oxides and their crystal structures taken from Kubaschewski and Hopkins[35] arranged in a pseudo-periodic table fashion. The oxides listed are those pertinent to most of the elevated structural materials for which increased oxidation protection is sought. Examination of the structures for a given periodic group, in light of the general rules that the only structures expected in compounds under pressure are those which are present for periodically similar compounds with larger cation/anion ratios, do not indicate that any novel structures are to be expected for these oxides.

2.6.2 Synthesization of New Compounds

Kaufman[27] describes the factors to be considered when attempting to synthesize new materials:

- Select the elemental system and composition region.

- Predict the crystal structure for the new material.
- Predict the lattice parameter and/or calculate the pertinent volume relationships.
- Predict the sign of the entropy change.
- Predict some of the general characteristics of the new materials and the magnitude of some physical or electronic properties.

At Manlabs[36] MoC was produced as a fcc structure at pressures of 35 to 90 kilobars at 2000°C. Normally Mo_2C is produced as a hexagonal structure at one atmosphere pressure. The stability of the high temperature structure was investigated by a short five minute temperature exposure at 1100°C, which did not result in the transformation of MoC to MoC + Mo_2C. However, a 1600°C exposure for five minutes did result in a transformation to a MoC + Mo_2C structure, a mixture of fcc and hexagonal crystal structures. This indicates that even though structures or compounds can be produced, one must still be limited by the kinetics of transformation back to a stable phase.

Recently, the synthesis of metal dioboride composites[37] was accomplished. This study illustrated the ability of hot pressuring techniques to manufacture a compound in a dense, crack-free body with a well controlled composition. Zr, Ta, Al, Si, and SiC were added to HfB_2 + ZrB_2 to form composites. The addition of SiC to HfB_2 and ZrB_2 gave the best oxidation resistance at 2200°K.

2.6.3 Alteration of Oxide Defect Structure

Work at the Westinghouse Research and Development Center[34] has demonstrated that vacancies can be removed from TiO and VO and that the high pressure structures can be retained upon return to atmospheric pressure. The vacancy concentration is completely removed from TiO and while (~5-10%) of the vacancies are removed from VO at 90,000 kbar-°C. NbO differs from TiO and VO in that the vacancy distribution in the NbO crystal structure is ordered. Because of this, the vacancy concentration in the NbO could not be decreased. TiO_2[38,39] has also been successfully compressed to remove vacancies.

The reduced defect structure has been retained upon depressurization to one atmosphere and cooling to room temperature. Unfortunately, for the purpose of this study, most of the work published in the field of high pressure technology has been directed toward the study of the effects of pressure and temperature on physical and thermodynamic phenomena and not toward the manufacture of stable or metastable structures for use at elevated temperatures. No information has been found which describes the stability after pressurization and vacancy removal.

2.6.4 Niobium Pentoxide-Candidate for High Pressure Exposure

The structure of α-Nb_2O_5 is a very open structure containing regular channels. The structure is built from NbO_6 octahedral units sharing corners and edges.[40] This fact immediately suggested the possibility of forming a denser phase upon the application of high pressures. No information was found in the literature concerning the effects of high pressure on any of the refractory metal oxides with the exception of NbO + VO. Therefore, high pressures were used to compact porous Nb_2O_5. By forming a dense equilibrium crystal structure of Nb_2O_5, the transport of oxygen through the structure could be decreased.

Chen and Swalin[41] have determined the diffusion of O in α-Nb_2O_5 to be described by the equation

$$D = 4.7 \times 10^{-3} \exp\left(\frac{-27{,}700}{RT}\right)$$

for the temperature range of 800 to 1150°C. Sheasby and Cox[42] have determined that the diffusion of oxygen in α-Nb_2O_5 is dependent on crystallographic orientation. They found that diffusion was two orders of magnitude more rapid parallel to the [010] direction as compared to diffusion perpendicular to the [010] direction for the oxide equilibrated at pO_2 = 10 torr. For an oxide with reduced stoichiometry, equilibrated at $pO_2 \simeq 10^{-17}$ atom, the anisotropy was evident, but to a smaller degree.

Based on the work of Gatehouse and Wadsley,[40] Nb_2O_5 is reported to be monoclinic, being composed of NbO_6 octahedral units sharing corners and edges. Sheasby and Cox[42] have reported this open structure to contain 2.3A° openings. In an open structure such as a-Nb_2O_5 with its probable covalent bonding it is possible that oxygen molecules could easily diffuse through the structure.

Kofstad[43] concludes that the defect structure of Nb_2O_5 could very easily be based on the presence of Nb^{2+} interstitial atoms at large deviations from stoichiometry (metal-excess) rather than mono-valent or di-valent oxygen vacancies as has been reported. These conclusions are reasonable, it is claimed, because of the effect of aliovalent impurities controlling the oxide vacancy concentration due to electroneutrality consideration being stronger than the effect of the equilibrium oxygen pressure on the vacancy formation.

Should molecules of oxygen be transported through the open structure instead of as charged particles, via the vacancy mechanism, disagreement between thermogravimetric and conductivity or resistance techniques for measuring transport properties could be the result of measuring different mobile entities.

This open structure and low density of Nb_2O_5 along with the possibility of oxygen transport being the result of molecular oxygen flow through holes in the structure immediately suggests that a more compact dense structure might be formed at high pressures and that this structure might decrease oxygen transport. If the transport of molecular oxygen through the open structure is the true mechanism and the defect structure of the oxide is cation interstitials, then the production of a new Nb_2O_5 structure could very greatly decrease the transport of oxygen to the surface of the material.

III. EXPERIMENTAL RATIONALE

Although many possible experiments had emerged during the course of the literature review, only three groups of experiments were selected to investigate techniques for modifying oxide defect structures to reduce the oxidation rate. The three experimental studies conducted were:

1. Influence of combined high pressure and high temperature on the structural form of Nb_2O_5. (This work was done by A. Taylor and N. J. Doyle at the Westinghouse Research Laboratories under an Astronuclear Work Order No. 59-R-Xa-19207.)
2. The effect of autoclave exposure on the oxidation resistance of Nb, Ta, and B-1 a niobium based alloy in air and oxygen at 20 mm Hg.
3. The effect of low pressure oxidation rates on the 1060°C oxidation rate of B-1.

3.1 High Pressure Study

This study was designed to determine if Nb_2O_5 could be transformed to a denser phase under elevated temperature and pressure conditions. An ideal experiment would be to grow an Nb_2O_5 film on a sample of niobium, compact the sample, and determine its effect on the rate of oxidation after compaction compared to the rate of oxidation for a control sample. However, the nature of high pressure research makes experimental techniques difficult and some of the unknown factors which could hinder the attainment of this goal are:

1. The compressability of the metal relative to the oxide could result in a compact, but non-adherent oxide.
2. The small sample size required to achieve large pressures will limit the kinds of evaluation which can be accomplished on a compacted sample.

For these reasons, it was more sensible to determine the effect of pressure on the structure of Nb_2O_5 as a single phase.

3.2 Autoclave Pretreatment

Based on the report of Nakayama and Osaka[11] where a rutile type structure on Ta_2O_5 was stabilized by Fe^{3+} ions during an autoclave exposure, the second set of experiments was made to determine if this mixed oxide, tapiolite, would have an effect on the oxidation behavior of Nb, Ta, and the B-1 alloy. Samples of the materials were exposed in an autoclave to form a tapiolite film and subsequently exposed to air at 1040°C and oxygen at 20 mm Hg at 650°C.

3.3 Oxidation Pretreatments

The third comparison involved the effect of a pre-oxidation exposure in 20 mm oxygen at 650°C on the air oxidation of a B-1 alloy. Pre-oxidation has been shown[6,7] to affect the oxidation behavior of materials. Therefore, the effect of a pretreatment on the oxidation behavior was investigated to determine why these treatments are effected. An understanding of how a pretreatment can improve oxidation resistance would lead to the ability to optimize such treatments.

IV. EFFECT OF HIGH PRESSURE AND TEMPERATURE ON THE STRUCTURAL FORMS OF Nb_2O_5

4.1 Experimental Material

Nb_2O_5 of purity > 99.995 (by the Kawecki Chemical Company) was employed. This was in the form of fine, well-crystallized powder which, by X-ray diffraction, was found to consist entirely of the stable high temperature α-form.

4.2 X-ray Technique

All diffraction patterns were taken at room temperature with a high intensity rotating anode X-ray tube using filtered Cr radiation and a Philips 114.6 mm diameter Debye-Scherrer powder camera. The positions of the X-ray lines for phase identification were obtained in the conventional manner using Nies charts, and the various phases were identified by means of the ASTM Data File and the d-spacing data presented in Terao's publications.[4]

4.3 High Pressure Technique

All high pressure runs were carried out in a tetrahedral anvil press of the Tracey-Hall type using pyrophyllite cells with tantalum heaters, and with the samples encapsulated in pure boron nitride cylinders. Pressures ranging from 10 to 78 kbar were employed in combination with temperatures ranging from room temperature to 1200°C.

The pressure-temperature cycle was one in which the sample was first taken to pressure. The heating current was then switched on and the sample heated for times ranging from 1 minute to 16 hours, after which the current was switched off, thereby effecting a rapid quench while the sample was still under pressure. The pressure was then gradually released. After removal from the press, the samples were finely powdered and subjected to X-ray diffraction analysis.

4.4 Results

The results are summarized in Table 4. Definite structural changes are observable due to the action of pressure alone or as the result of pressure and temperature in combination.

Under pressure alone, the stable α phase retains its structural identity and original white color up to a pressure of 56 kbar, but at 67 and 78 kbar there is a progressive change to an as yet unidentified structural modification.

Heating untreated material to 1200°C retains the α form, but 1 minute at 10 kbar + 1200°C converts α to a mixture of Terao's γ + Mod II forms,[4] whereas after 5 minutes it is all converted to the γ form.

Increasing the pressure further at 1200°C to 56 and 78 kbar, yields at room temperature, a mixture of the γ + γ' forms. It is not certain whether a mixture of forms existed at pressure + temperature, or whether γ formed from γ' during the course of the quench.

At 400°C + 56 kbar a mixture of α + γ is produced, but on raising the temperature to 800°C only a trace of α is visible.

4.5 Discussion of the Results

Nb_2O_5 can be prepared in a large number of closely related structural forms, only a few of which have been completely investigated. A detailed review of the preparation of the oxide and its structures, covering work to the end of 1968, is given in "Gmelin's Handbuch der Anorganische Chemie" [(Verlag Chemie GMBH.) Niob, Teil B1, System Nummer 49, 1970, pages 45-78]. Table 5 which is based on Gmelin, summarizes the nomenclatures used by several authors for the various crystallographic forms. For convenience, we shall use the nomenclature used by Terao (Ref. 4) because the structural data in the form of interplanar spacings and intensities obtained in the course of the present investigation conform most closely to Terao's findings.

There is some evidence to indicate that under certain oxidizing conditions, there will be a slight departure from the stoichiometric composition Nb_2O_5. The lower limit of the Nb_2O_5 phase at 1300°C has been given as $Nb_2O_{4.878}$ and $Nb_2O_{4.887}$ at 889°C. According to Goldschmidt[46] there is some evidence to show that of all the forms, the most stable one is the monoclinic α form which is produced by oxidizing powdered niobium metal in air at 700-800°C. Table 6 lists a number of structural forms of Nb_2O_5, based on the compilation by Terao.[4]

As shown by Terao, heating niobium metal in air at 300-350°C gradually converts it, via a number of structural forms, to the monoclinic γ form listed in Table 6. Further heating in air or at the reduced pressure of 10^{-1} to 10^{-3} torr, and at temperatures ranging from 750 to 900°C converts γ to the stable high temperature monoclinic α form via the following sequence of stages:

$$\gamma \rightarrow \gamma' \rightarrow \beta \rightarrow \alpha$$

These structures are closely related, the changes being effected essentially by a redistribution of the niobium atoms among the available sites between the oxygen atoms. For this reason, as a consideration of the unit cells in Table 6 will indicate, the monoclinic angle is always close to 120°, and the following relationships will be seen to exist between the forms:

$$a(\gamma) \approx a(\gamma') \approx a(\beta)/3 \approx a(\alpha)/3;$$
$$b(\beta) \approx 2b(\alpha);$$
$$c(\beta) \approx c(\alpha), \text{ etc.}$$

If Nb_2O_5 is mixed with metallic Nb and heated in vacuum at 750°-1000°C, a reaction occurs in which Nb_2O_5 is gradually converted to NbO_2, in accordance with the equation

$$2Nb_2O_5 + Nb > 5NbO_2$$

The reaction proceeds by the slow diffusion of niobium atoms into the crystalline cell of Nb_2O_5. This leads to the formation of an intermediate monoclinic structure to which the formula $Nb_{12}O_{29}$ ($Nb_2O_{4.83}$) has been ascribed. This is Terao's Modification II, which is listed in Tables 5 and 6.

The few experiments listed above and summarized in Table 4 indicate that the combined effects of temperature and pressure will produce significant changes in the crystal structure of Nb_2O_5. Much more work would be required to draw a proper P-T phase diagram for the compound Nb_2O_5.

It is significant that the conversion of the stable high temperature α-form to the γ form by the combined action of temperature and pressure is accompanied by an increase in density from 4.56 to 5.815 gram/cm^3. Such an increase in density could have a beneficial effect on the corrosion-resistance properties of a niobium-rich alloy which is subjected to high temperature conditions.

Terao has shown that the γ form is produced by heating the low temperature δ modification in the temperature range 400-700°C and, based on density measurements, attributes to it possible formulae $Nb_{28}O_{70}$ (= 14 Nb_2O_5) and $Nb_{28}O_{69}$ ($Nb_2O_{4.928}$). These correspond respectively to oxygen contents of 30.10 wt % for $Nb_{28}O_{70}$ and 29.79 wt % for $Nb_{28}O_{69}$. Thus, in order to distinguish, by gravimetric analysis, these two stages of oxidation, the precision would have to be better than 0.1%.

The present investigation shows that the high temperature α form is completely converted to the lower temperature γ-form by heating to 1200°C at 20 kbar. We may therefore raise the question as to whether oxygen is lost in the process in accordance with the reaction

$$Nb_{28}O_{70}\,(\alpha) \xrightarrow{1200^\circ C\ +\ 20\ kbar} Nb_{28}O_{69}\,(\gamma) + 0.$$

A sample of γ-phase produced as above and weighing 0.013139 grams was heated in air for 1 hour at 1000°C and converted completely to the α form. A gain in weight of 0.000058 grams was expected if an oxidation process was involved. No gain in weight was observed. Since the precision of the balance employed was 0.000005 grams, the expected gain would easily have been detected. We can therefore state that the γ form can exist at the stoichiometric composition Nb_2O_5, without ruling out the possibility of the structure existing over a range of composition, namely from $Nb_{28}O_{69}$ to $Nb_{28}O_{70}$.

The β-phase given by Terao in the sequence $\gamma \longrightarrow \gamma' \longrightarrow \beta \longrightarrow \alpha$ was not found in the high-pressure series of experiments. Further exploration of the P-T diagram would be necessary to uncover its range of existance.

V. PRETREATMENTS AND OXIDATION BEHAVIOR

5.1 Experimental Materials

The test samples were cut from double electron beam melted tantalum and niobium plate which was rolled to .075 cm (.030 in.) thick sheet. The B-1 alloy was argon-arc melted and processed to sheet as reported in Reference (6). All samples were polished through 600 grit silicon carbide paper and vacuum annealed at 1200°C for 1 hour. All samples tested in oxygen and air were cleaned with acetone and ethyl-alcohol prior to exposure.

5.2 Autoclave Exposure Procedure

One set of samples was submitted to the Nuclear Energy Division Test Engineering Group for exposure in an autoclave. These samples were cleaned by the autoclave operators just prior to exposure to eliminate contamination during handling.

The pure niobium, pure tantalum and a B-1 niobium alloy samples were exposed in water in an autoclave at 350°C (660°F) for 16 to 20 hours at 2900 psi. Ferric (Fe^{3+}) nitrate ($Fe(NO_3)_3 \cdot 9H_2O$) was added to Grade A, demineralized water to obtain a .075 mg/100 ml (.75 ppm) ferric ion concentration as a starting point. The initial oxygen concentration of the solution was reported to be 8.54 ppm, while the post test oxygen concentration analysis indicated that the oxygen level had been reduced to 0.101 ppm. The solution used in the autoclave had a resistance of 87,400 ohm/cm, a pH of 4.72 units, and a chloride ion concentration of < .02 ppm as compared to the specifications for Grade A water listed in Table 7.

The samples were suspended from the sample holder "tree" by preoxidized stainless steel wires. The system was then loaded with the samples and enough solution was added to form a single liquid phase autoclave environment, commonly termed a "solid" autoclave. The autoclave was heated to a temperature of 350°C at the rate of about 30°C/hr., and was maintained at that temperature for 16 hours. The pressure in the system was maintained at about 2900 psia.

Following the autoclave exposure, the system was cooled down and the liquid sampled for post test chemical analysis of the oxygen concentration. After the autoclave exposure, samples were handled with gloves to prevent contamination or injury to the coatings.

5.3 Oxidation Apparatus and Procedure

Two experimental apparatus were used to evaluate oxidation behavior. The Cahn High Vacuum Microbalance System was used to evaluate oxidation behavior at 20 torr and to pretreat the B-1 alloys. The Stanton Thermobalance was used for all air oxidation testing at 1040°C.

5.3.1 Cahn Microbalance

The experimental apparatus is shown schematically in Figure 3. The entire apparatus was constructed from stainless steel and quartz with copper gasket seals. The system was completely bakeable. A brief description of the components follows.

Furnace: A vertical non-inductively wound, resistance heated Lindberg Hevi-Duty Clam Shell Furnace having a 24-inch long heater element with a 6-inch long constant temperature zone was used to heat the sample. The reaction chamber in the furnace was constructed from a 38 mm quartz tube attached to the system via glass-metal seals and stainless steel bellows.

Temperature was measured using a Pt-Pt/13Rh thermocouple suspended in the vacuum system. The bead of the thermocouple was shielded from direct radiation by an alumina protection tube. The temperature was corrected for position and radiation effects by comparison with thermocouples directly attached to a sample in the hot zone during a separate calibration run.

Balance: Continuous weight change measurements were made using a Cahn UHV-RH microbalance with a 100 gram capacity and a 2 microgram sensitivity.

The balance was housed in a stainless steel chamber constructed from a standard 8-inch Varian flanged nipple. Varian 2-3/4 inch nipples were cut and welded to the 8-inch nipple to provide appendages for the sample and counterweight hang downs and for thermocouple feedthroughs. The microbalance was mounted on a standard Varian rotatable 8-inch blankoff along with the vacuum feedthrough containing the electrical connections for the balance. The samples were suspended from the balance by 2 mm diameter quartz rods.

Weight changes were continuously recorded on a dual pen recorder with a potentiometric input system. A one mv full scale recorder range was used for all continuous weight-gain records.

Pumping System: The apparatus was evacuated with a 4-inch diameter Freon trapped diffusion pump, using silicone oil as the pumping fluid.

Gas: Baker ultra-high purity oxygen was used directly from the cylinder and admitted into the system via Varian leak valves.

Pressure Measurement: The oxygen pressure was measured using a standard U-tube mercury manometer with one end open to the atmosphere.

Experimental Procedure: The samples were loaded into the furnace tube and the system was evacuated to 10^{-6} torr before the sample was heated. Heating to the testing temperature of 650°C was accomplished in 30-45 minutes. After soaking for 15 minutes, the vacuum pump was isolated from the system and the oxygen was admitted via a variable leak valve until a pressure of 20 torr was read on the Hg U-tube manometer. The system was sealed and the rate of oxidation was measured by continuously recording the rate of weight change. The total system volume was over 6 liters and less than one torr pressure decrease was detected. An initial weight correction was made to compensate for the weight loss on heating resulting from the desorption of the adsorbed molecules on the quartz bang down rod.

5.3.2 Stanton Thermobalance

The oxidation testing in air was done using a high temperature model Stanton Thermobalance. Heating was accomplished in a vertical platinum/rhodium wound furnace, with the natural convection current providing a fresh supply of oxygen. Temperature was controlled to within $\pm$ 2°F by the output of a platinum-platinum/rhodium thermocouple. The weight increase could be determined within $\pm$ 1 mg. Both weight and temperature were continuously recorded. The test samples were supported in a Coor's porcelain crucible with the sheet samples held in a vertical plane by slots cut into the lip of the crucible with a diamond saw. For the temperatures and environments under consideration, no discoloration or other reaction was noticed.

The samples were loaded onto the balance arm while the furnace, poised above the sample was heated to 1060°C. When the furnace was at temperature, the furnace was lowered over the sample. In less than 2 minutes, the sample was at temperature. The initial weight of the sample was corrected for the weight loss of the empty crucible mounting system due to adsorbed moisture being lost. Since the furnace tube was in the vertical position, air was continuously supplied to the sample via convection. Weight gains were continuously recorded.

5.4 Results

5.4.1 Autoclave Exposure

After the 16 hour run in the autoclave the samples were weighed. The tantalum samples gained 87 $\pm$ 7 $\mu g/cm^2$, the niobium samples gained 135 $\pm$ 10 $\mu g/cm^2$ while the B-1 samples gained 40 $\pm$ 5 $\mu g/cm^2$. The macroscopic appearance of the samples after the autoclave exposure are shown in Figure 4. It is interesting to note that although tantalum has a larger affinity for oxygen than does niobium, the niobium samples gained more weight during the exposure, indicating that the ferric ions play an important part in the reaction of niobium and tantalum with the autoclave environment. The thin films formed on the surfaces of the samples was not detectable even on 1000X oil immersion photo micrographs.

The oxide films formed on the samples were examined using both a Siemens 114 mm diameter powder camera and a Siemens x-ray diffractometer. The results are summarized in Table 8 and a positive of the powder pattern film is shown in Figure B1, Appendix B. The white area near the hole in the film is the result of the fluorescence of Fe in Cu K radiation. Table A1 in Appendix A lists the estimated relative intensities and the d-spacings of the oxide films formed during the autoclave exposure.

The tapiolite phase (Fe (Ta, Nb) O) was produced on all of the samples by the autoclave exposure. However, a number of additional oxides of Nb and Ta were formed. This is probably the result of a rapid depletion in the Fe content of the solution; only 0.75 ppm of the ferric ion was added, whereas, 8.54 ppm of oxygen was initially present in the solution.

5.4.2 Oxidation Behavior

A summary of the oxidation experiments are listed in Table 9. Weight gain (mg/cm^2) as a function of time, the visual description of the oxides, x-ray analysis of the oxides, and metallographic studies of the oxide and oxide-substrate system are presented for the systems and conditions studied.

5.4.2.1 Nb Oxidation

Figures 5 and 6 compare the short time oxidation behavior of pure niobium and autoclave exposed niobium in air at 1 atm and 1060°C and in oxygen at 20 torr and 660°C respectively. The autoclave exposure actually increased the rate of weight gain of niobium in air; this oxide formed in 2 layers, a thin light yellow layer on the exterior of the normally white Nb_2O_5. In 20 torr O_2, the autoclave exposure decreased the initial rate of weight gain, but after about 30 minutes, the rate of weight gain was equivalent to that of the unexposed niobium.

The results of an x-ray analysis of the oxides formed during runs 10 and 12 (Figure 5-niobium in air) are shown in the Appendix, Figure B-2 and Table A2. The film 12q is the pattern

produced by a yellow outer oxide layer formed on the autoclave exposed Nb during air oxidation. All of the oxides show identical patterns and the best fit is provided by comparison to ASTM card 15-493. The only apparent difference in the films is the darker 12q film probably due to the fluorescence of Fe in Cu Ka radiation. Both oxides were fairly adherent to the metal substrate on the large flat surface of the samples, however spalling occurred on cooling at all edges and corners. Also, the oxides on both samples exhibited a layered structure and these layers were partially coherently.

The initial oxidation behavior in air shown in Figure 5, for niobium with and without a tapiolite film was characterized by a short period of parabolic behavior followed by a linear to increasing rate of oxidation with time and then followed by an apparent decreasing rate of oxidation with time. The oxidation of Nb in air forms stable NbO, and NbO_2 oxides, as well as the pentoxide Nb_2O_5. It has been shown that there is a minimum in the curve of the linear rate constant vs. temperature for niobium, at one atmosphere oxygen, this minimum occurs at $\sim 820^{\circ}C$ and the minimum occurs at higher temperatures as the oxygen pressure decreases to 10 torr oxygen, the minimum occurs at between 1050 and $1100^{\circ}C$ but is less pronounced.[52] It is not certain what produces this minimum, but it is possible that the Fe addition to the scale might affect the same mechanisms which account for this minimum.

Run No. 1 and 2 were untreated niobium samples. Sample 1 was initially heated to temperature in a 10^{-3} torr roughing pump vacuum while Sample 2 was heated to temperature in a 10^{-6} torr vacuum. The oxide on Sample 1 was white-gray in appearance, while Sample 2 was blue-gray. The blue-gray oxide was much more adherent than the oxide on Sample No. 1. Sample 7, pre-exposed in the autoclave had a green-brown appearance and the same texture and adherence as the oxide on Sample 2. The x-ray results showed no difference between the scales. However the x-ray patterns derived from these niobium oxides best fit the indexed lines for β-Ta_2O_5 (ASTM card 19-1298). It is absolutely certain that these samples were niobium oxidized in 20 torr oxygen. Therefore, the Nb_2O_5 grown under these conditions

must be iso structural with β-Ta_2O_5. The x-ray powder films are shown in Figure B-3 and the relative intensities and d-spacings are shown in Table A3. The oxide film formed on the pure niobium did cause a decrease in the oxidation rate for the first several minutes. This would indicate that initially the reaction of oxygen with the Nb was somehow impeded either by diffusing slower through the autoclaved film or by reacting initially with the autoclaved film, thereby using up oxygen.

5.4.2.2 Tantalum Oxidation

Figures 7 and 8 compare the short time oxidation behavior of pure tantalum and tantalum exposed in the autoclave in air at 1060°C and in oxygen at 660°C respectively. As in the case of pure niobium, the sample treated in the autoclave actually oxidized faster in air than did untreated tantalum. The oxide also formed in 2 layers with a thin light yellow oxide on surface and the standard tantalum oxide beneath. There was little or no difference in the oxidation behavior between the autoclaved exposed sample in oxygen at 20 min. Hg. Figure B4 and Table A4 show the x-ray powder patterns and the d-spacings for the oxides formed on the tantalum.

The x-ray results of the films formed on samples from Run 9 and 13 show very similar structures. The patterns are best fitted with a monoclinic β-Ta_2O_5 (ASTM card 19-1298) and an orthorhombic Ta_2O_5 (ASTM card 8-255). The oxide layer on the pure tantalum had a mottled white-gray appearance but the oxide scale was very tightly adherent to the flat surfaces of the sample. Only at the corners and edges did spalling occur. The sample of tantalum exposed in the autoclave has a yellow outer surface with a light brown mottled area. The center of the oxide layer was white while the surface which was adjacent to the metal had a mottled gray appearance as did the surface of the tantalum. This scale was non adherent and flaking of the oxide occurred over about 75% of the total surface area. If one utilizes the schematic rate equation summary for tantalum as presented by Kofstad,[53] the oxidation of tantalum in air at 1060°C proceeds by two different mechanisms. Initially during oxidation

from 800°C to 1250°C a parabolic (II) oxidation takes place. This is noted in both samples on Figure 7 for the first 5-10 minutes. This behavior is attributed to the fact that TaO_z is no longer the intermediate reaction product in this temperature range. TaO_z is replaced by TaO as the intermediate reaction product in the reaction scheme.

Ta-O soiid solution $\longrightarrow$ (TaO) $\longrightarrow$ β-Ta_2O_5 the parabolic (II) stage then corresponds to the formation of a compact scale of β-Ta_2O_5 through which oxygen must diffuse and is thus rate determining.

Following the parabolic (II) stage in the temperature range from 800°C to ~1050°C is the linear (II) stage during which the protective properties of the scale are broken down by repeated cracking of the scale. Both Sample 9 and 13 exhibit the parabolic II behavior and, for the experimental times, appear to be in the linear (II) stage. It appears that initially the film on Run 13 allows oxygen to diffuse faster through the β-Ta_2O_5 and then finally, the plastic and adherent properties of the film are subsequently impaired as indicated by the spalled oxide on Run 13 as compared to the adherent oxide on Run 9 and the faster linear (II) rate; 1.03 mg/cm^2/min. to .542 mg/cm^2/min. for untreated tantalum.

Tantalum samples were also oxidized in 20 torr oxygen, Run 14 and 8. The oxide formed in Run 14, which had been exposed in the autoclave appeared as tan-brown and gray mottled oxides having the appearance of forming tan islands on a gray field. Immediately below the tan surface, the oxide was similar to the untreated oxide. The untreated tantalum was a mottled white gray appearance with the same features as the sample from Run 14. Oxides were adherent on both of the samples.

The film formed on the tantalum by the autoclave exposure had no effect on the oxidation behavior of the metal compared to a non-exposed sample. The x-ray powder patterns showed poorer resolution and broader lines for the oxide grown in 20 torr oxygen than for the oxide formed in air. This probably resulted from the oxide being slightly oxygen deficient as the result of the lower pressure oxidation.

5.4.2.3 B-1 Niobium Alloy Oxidation

Figure 9 shows the oxidation behavior of autoclaved B-1 and regular B-1 sample oxidized in air at 1060°C and in oxygen at 650°C and 20 min. Hg. For Runs 11 and 16, the rate of oxidation in air is similar up to about 100 minutes, at which time the sample exposed on the autoclave begins to oxidize at a slightly faster rate. The rate of oxidation in 20 torr O_2 was exactly similar as is noted for Run 17 and 18 on Figure 6.

The most interesting result, however, is the effect of either a pre-oxidation in 20 mm Hg of oxygen at 650°C or an autoclave treatment plus the 20 mm Hg O_2 pre-oxidation at 650°C. Samples 17 and 18 were oxidized in air after the 20 torr exposure. Both of these treatments resulted in a reduced oxidation rate for the times tested when compared to the respective alloys in the non pre-oxidized state. The x-ray results for the B-1 alloys are shown in the Appendix, Figure B5 and Tables A5 and A6. Figure 10 shows the appearance of the samples from Runs 11, 16, 19 and 20. Samples 16 and 19 were not exposed in the autoclave. Sample 16 was oxidized only in air while Sample 19 was first pre-oxidized in 20 mm O_2. The oxides on both of these samples is white. The oxides formed on the autoclave exposed samples were yellow on the surface. The oxide on Sample 16 spalled at the edges, but was impossible to scrape the oxide from the flat surface. Figure 11 shows the oxide metal interface of the polished samples. Note the grain boundary extensions in the oxide as well as the preferential grain boundary attack in the affected zone. When these same samples were lightly etched, Figure 12, a third affected zone was revealed along with a darkened interface between the matrix and the newly revealed affected zone. Also, precipitate particles, possibly the result of internal oxidation in the matrix, were revealed. Also evident is a selected staining of the grains in the affected zone. The etch was a 1:1:1 mixture Glycerin, HNO_3 and HF.

The autoclave exposure alone had no effect on the oxidation of these alloys in air. However, a pretreatment in 20 mm Hg for 280 minutes for Samples 19 and 240 minutes for Sample 20 resulted in a decrease in the parabolic rate constant by a factor 2.

While many emperical studies have been made on the effects of alloy additions on the oxidation rate of niobium alloy, little is understood about the mechanisms involved in the protective properties of the oxide scales on niobium alloys. In looking for differences in the oxides formed on the Samples 11 and 16 and Samples 19 and 20, the oxide and substrates were examined metallographically and both x-ray diffractometer and powder patterns were made on the oxides. No easily discernable differences were noted. The macroscopic surface was mottled for the samples exposed to the lower pressure oxygen and the macroscopic cross section of the oxide scales indicated a slightly less porous oxide structure, although this is difficult to characterize quantitatively. The main differences were in the x-ray diffraction patterns, particularly the intensity of the 3.20 line on the diffractometer measurements. This line is the primary line for TiO_2 and is not shared by the other oxides which have been fitted. This would indicate that TiO_2 (rutile) forms preferentially on the B-1 alloy exposed in air. However, the secondary lines for TiO_2 2.20, 2.30, and 2.495 are larger for the samples exposed in 20 torr oxygen. It is not possible to ascertain at this point whether these latter lines are the result of intensity enhancement by other oxides or because of the preferred orientation of the oxide in the scale on the metal substrate. Microprobe examination of the effected zones could possibly indicate the preferential oxidation TiO_2 in air as opposed to some other oxide when exposed to 20 torr oxygen. A diffractometer trace of the oxide formed on the Sample No. 20 after pre-exposure to 20 torr oxygen, but before exposure to air gave only 3 very broad and ill defined peaks indicating either some very small particle oxide or an amorphous type of a compound on the surface. Typical oxygen pickup for the B-1 alloys in 20 torr oxygen was only about 500 $\mu g/cm^2$ in 3.75 hours. Without further investigation, it is difficult to determine the cause of the improved oxidation resistance of the B-1 alloy by pre-exposure to 20 torr oxygen at 650°C. Neither can it be determined from the samples tested whether or not these are the optimum pre-exposure conditions. Sample 11 and 20 were autoclave exposed. As a result, the surfaces of these samples are tinted yellow. The micrographs in Figure 11 reveal the same features for these samples as was noted for Samples 16 and 19. The surface texture of Samples 19 and 20 appear mottled or coarse when compared to Samples 16 and 11.

A very quick qualitative election microprobe analysis was made on Sample 11 by scanning the edge of the sample. Visual examination of the darkened edge from which the oxide had spalled revealed three distinct layers. These layers were scanned with the following results.

(1) Fe was present at the yellow surface of the sample but decreased as one moved to the exposed under layers.

(2) Tantalum, W, and Nb concentration decreased as one proceeds from the metal to the outer oxide layers.

(3) The Ti concentration was irregular, as if distributed in islands in the metal and the first oxide layer, but appeared to have a lower but more evenly distributed concentration on the outer layer.

VI. GENERAL DISCUSSION

Many techniques for enhancing oxidation protection have been reported; alloying, coating, pretreatments, oxide phase stabilization techniques, heat treating of scales, and the application of potentials across scales.

Alloying, by far the most ideal approach, is done to provide components which will selectively oxidize to form protective scales. To be protective, scales must have a slow transport rate for the cation or anions responsible for oxidation. The scales must also adhere to the metal and the stresses caused by differential thermal expansion must be accommodated by the oxide by plastic deformation in the oxide. The other alternative would be to somehow invent a scale with the same thermal expansion rate as the metal. An oxidation resistant alloy has the advantage that should a defect occur in the scale during operation, the components needed to form the scale are present in the alloy and a new protective scale can form.

In the refractory metal systems, the structural alloys possessing sufficient high temperature strength can be clad with a more oxidation resistant alloy. Work at IITRI[54] has been involved with the development of a Hf-Ta base alloy system to clad structural Nb alloys. Work at Solar[55] involves the use of a Nb-42Ti-9Cr-4Al alloy as a ductile matrix which surrounds W-alloy fibers. In the case of an Hf-Ta based alloy, a thick oxide scale is formed consisting of oxides of the form $6AO_2 - B_2O_5$ where A is a Group IV-B metal and B is a Group V-B metal. The exception to this appears to be the $TiO-Nb_2O_5$ system.

The oxide system that grows on the B-1 alloy is also composed of the $TiO-Nb_2O_5$ mixed oxide system. As was shown, a pre-oxidation exposure enhanced the protectiveness of the scale formed. Two possible causes for this enhancement are suggested. The first is the growth of a new oxide with lower transport rates for oxygen, and second is the formation of an oxide which was able to accommodate the growth stresses which arise when n-type oxides grow at the alloy oxide interface. Research is now being done to understand the reasons for the mechanical breakdown of scales and films, and to determine what can be done to enhance the plasticity of the films growing on the alloys.[56]

However, in spite of the research effort, the ideal strong ductile oxidation resistant alloy has not been developed. Dupont has patented a series of Nb containing alloys that appear to possess the proper oxidation properties, however, these alloys contain large amounts of Al, Co, Fe, and Ni which tend to render the alloys unusable because of production and fabricability difficulties. It appears that these alloy additions form protective oxides by stabilizing a NbO_2 structure and/or forming intermetallics such as $CbAl_3$ in the oxide system which have reduced oxygen transport properties.

Although there is a vast quantity of data available concerning the oxidation behavior of many alloy combinations, little effort has been made to determine if any mixed oxides containing Nb have transport rates which are slow enough to be an effective oxidation barrier if the scale could be grown and made stable, plastic and adherent. There are data available for the diffusion anions and cations through many single oxides, spinels, and other oxide mixtures, and it is possible from this information to eliminate certain systems and be encouraged to investigate other systems. However, outside of the diffusion rate measurements for oxygen in Nb_2O_5, no data can be found for the transport properties of mixed niobates. An investigation of such behavior would help research workers to focus on alloys and coatings which will show definite promise.

From the results of this study it is currently impossible to estimate the potential value the techniques of pre-oxidation and high pressure in the stabilization and formation of protective oxide structures. Because of the complexity of multi-component alloy oxidation processes, it is very difficult to pre-determine the effect of an optimum pretreatment condition for example on alloy B-1. In a complex oxide-complex alloy system, the oxides formed by pretreatment could revert to some less desirable equilibrium condition on exposure, or the oxide system could remain protective. Our understanding of the complex interactions within these systems is so small that it is not possible at this point in time to intelligently design an oxidation resistant refractory metal alloy.

VII. CONCLUSIONS

Pretreatments show promise of being able to selectively form protective seals on the surface of an alloy. This has been demonstrated in this program for the B-1 niobium alloy, but the principles and treatments involved can be adapted to other alloys. Work is needed to understand the mechanisms responsible for this enhancement in oxidation protection so that pretreatment processes can be designed for a given alloy. Although little effect was found as a result of the autoclave pre-exposure, the feasibility of forming films on the surface of materials by this technique has been demonstrated.

High pressure techniques are able to change the structure of oxides. For Nb_2O_5 studied in this program an increase in the density of the structure was achieved. Questions concerning the stability of the high pressure oxides remain to be answered as do questions concerning the effect of binary oxide additions on stabilizing the protective structures produced by the high pressure treatment.

Now that it has been demonstrated that pre-oxidation does have an effect on oxidation rates, the potential magnitude of this effect should be determined for refractory metal alloys. This involves understanding the factors which affect the oxidation behavior, such as the reaction rates of individual alloying elements under pre-oxidation conditions, the transport properties of the participating species, i.e., alloying element and oxygen in the metal and cations, anions, and electrons in the scale.

VIII. RECOMMENDATIONS

Some of the questions which should be answered by future study and which look particularly fruitful as the result of this program are:

(1) What are the optimum conditions for the formation of protective films as the result of low pressure pre-exposure and what is the extent of this long term protectiveness.

(2) What phase or phases, or what other quality of the oxide produced during pre-exposure causes the improvement.

One important area that will be examined during the 1971 program is the transport kinetics of the existing oxides. If an oxide is made to be adherent and stable, then the limiting factor controlling the rate of oxidation is the rate of transport through the oxides. A great many potential systems can be readily eliminated from consideration by transport kinetics which are too rapid. On the other hand, a measurement of transport kinetics in oxides can be used as a technique for screening potential systems. Many super alloys form spinel type oxide scales through which transport of anions and cations is very slow. However, there is little information concerning the transport properties of mixed refractory metal oxides. An investigation of the transport behavior of these oxides would give direction to investigators in pursuing further work.

The transport of oxygen through Al_2O_5, Cr_2O_3 and SiO_2 is slow enough to provide good protection for the oxidation of refractory metals, if these oxides can be caused to adhere and remain intact during the use of the component. These oxides are responsible for the protectiveness of many of the coatings developed to date. A detailed study of the compounds which mate these protective layers to the structural member will increase the possibility of optimizing a particular coating to a specific alloy.

IX. REFERENCES

1. Kofstad, P., "High Temperature Oxidation of Metals," John Wiley & Sons, Inc., New York, 1966.

2. Hauffe, K., "Oxidation of Metals," Plenum Press, New York, 1965.

3. Kubaschewski, O., and Hopkins, B. E., "Oxidation of Metals and Alloys," Butterworths London, 1967.

4. Terao, N., Japan Journal Applied Physics, V4 (1965) 8; V2 (1963) 156.

5. Brauer, G. Z. Anorg. Allg. Chem. V248 (1941) 1.

6. Cornie & Goodspeed, AFML-TR-69-64, Development of Ductile Oxidation Resistant Columbium Alloy, July, 1969.

7. WANL unpublished data.

8. Tedmon, C. S. and Hagel, W. C., J. Electrochemical Society, Vol. 115, No. 2, Feb. 1968, pg. 147.

9. Bhat, T. R., and Khan, I. A., J. Less Common Metals, VII 1966 pg. 290.

10. Geschwind, G., Scripta Metallurgica, Vol. 2, 1968, pg. 519-524.

11. Nakayama, T. and Osaka, T., J. Less Common Metals, Vol. 13, No. 3, 1967, pg. 360.

12. Goldschmidt, H. J., "Interstitial Alloys," Plenum Press, New York, 1967, pg. 419-422.

13. Spretnak, J. W. and Speiser, R., "Protection of Niobium Against Oxidation at Elevated Temperatures" RF Project 467, Report 16. Contact N6 Ohr-225(28) (NR 039-005).

14. Kofstad, P. K. and Hed, A. Z., Journal of Oxidation, Vol. 2, No. 1, 1970, pg. 101.

15. Private Communication G. Sabol, Westinghouse Research and Development Center.

16. Mendel, J. M. and Pollack, S. R., J. Phys. Chem. of Solids, Vol. 30 (4) 1969, pg. 993-1001.

17. Gibbs, G. B., Phil. Mag., Dec. 1968, V. 18 (156) 1175-1180.

18. Uhlig, H. H. and Brenner, A. E., Acta Met. V3, (1955) 108.

19. Cismaru, D., and Cismaru, G. D., Proceedings of the 1st International Congress on Metallic Corrosion, Butterworth, Science Publ. 1962, 237.

20. Lawless, G. Wm., and Lombard, C. A., AFML-TR-65-412, AFSC, WPAFB, Feb. 1966 (Available from DDC as AD-482570).

21. Schein, F., LeBouchu, B., and Lacombe, P., Compt. Rend. Acad. Sci., V 252 (1961) 4157.

22. Jorgensen, P. J., J. Chem. Phys., V. 37, (1962) 874.

23. Jorgensen, P. J., Electrochemical Soc., V. 110 (1963) 461.

24. Zaplatynsky, I., NASA-TN-D-4240 (1970).

25. Berkowitz-Mattuck, Joan. B., "Effect of Applied Electric Fields on the Mechanisms of Oxidation of Metals and Alloys" NASC, Contract No. N00019-70-C-0249,1970.

26. Kaufman, L., "Phase Equilibria and Transformations in Metals under Pressure," Solids Under Pressure, Ed. Paul and Warschauer, McGraw-Hill, New York, 1963, pg. 304.

27. Kaufman, L. and Clougherty, E. V., "Thermodynamic Factors Controlling the Stability of Solid Phases at High Temperatures and Pressures," Met. Soc. Conf. No. 22, Vol. 22, 1964, pg. 322.

28. Rooymans, C. J. M., "The Behavior of Some Groups of Chalcogenides under Very High Pressure Conditions," Advances in High Pressure Research, Academic Press, London, Vol. 2, 1969, Ed. by R. S. Bradley.

29. Neuhaus, A., (1964) Chemia V18, pg 93.

30. Goldschmidt, V. M., (1926) Skr. Norske. Videusk. -Akad. V. 2, No. 1

31. Rooymans, C. J. M., Ibid, No. 3, pg. 4.

32. Coes, L. (1953) Science V 118, 131.

33. Kulcinski, G. L. and Maynard, J., Applied Physics, Vol. 37, No.9, (1966), pg. 3519.

34. Taylor, A. and Doyle, N. J., "Vacancy Filling in Titanium Monoxide," Scientific Paper 68-154-PRESS-PS, Westinghouse Research and Development Center, January 14, 1970.

35. Ibid, Ref. 3, pg. 8-12.

36. PB181111 - Research and Development on High-Pressure, High-Temperature Metallurgy, Aug. 1961.

37. Clougherty, E. V., Pober, R. L., and Kaufman, L., TAIME Vol. 242, June 1968, pg. 1077.

38. Vahldrek, F. W., Journal of the Less Common Metals, V. 11 (1966) pg. 99.

39. Vahldrek, F. W., Journal of the Less Common Metals, V. 14 (1968) pg. 133.

40. Gatehouse, B. M. and Wadsley, A. D., Acta Crystal, 17 (1964) 1545.

41. Chen, W. K. and Swalin, R. A., J. Phys. Chem. Solids, V. 27, (1966) pg. 57.

42. Sheasby, J. S. and Cox, B., J. Less Common Metals, V. 15, 1968, pg. 129.

43. Kofstad, P., J. Less Common Metals, V. 14, 1968, pg. 153.

44. Vaisnys, J. R. (1967), J. Applied Physics, V. 38, 2153.

45. Wilhelmi, Karl-Axel, Acta Chemica Scanden Avica, V. 22, (1968), pg. 2565-2573.

46. Goldschmidt, N. J., J. Inst. Metals 87 (1959) 235. β, α. 0.

47. Kubaschewski, B. E. Hopkins, J. Less Common Metals 2 (1960) 172.

48. (a) ζ, η. F. Laves, R. Moser, W. Petter. Naturwissenschaften 51, (1964) 356.

(b) F. Laves, W. Petter, H. Wullf. Naturwissenschaften 51, (1964) 633.

(c) δ or γ', γ, β or α', α. F. Holzberg, A. Reisman, M. Berry, M. Berkenblit. J. Am. Chem. Soc. 79 (1957) 2039.

(d) A. Reisman, F. Holtzberg. J. Am. Chem. Soc. 81 (1959) 3182.

(e) γ, β, α. R. A. Zvinchuk, Kristallografiya, 3, (1958) 744.

(f) δ, γ, β, α. R. Moser Schweiz. Mineral. Petrog. Mitt. 45 (1965) 35.

49. H. Nowotney, F. Benesovsky, E. Rudy and A. Wittmann, Monatsh. Chem. 91 (1960) 975.

50. M. W. Shafer and R. Roy, Z. Krist. 110 (1958) 241.

51. G. Brauer, Z. Anorg. Allg. Chem. 248 (1941) 1.

52. Ibid 1, pg. 217.

53. Ibid 1, pg. 191.

54. Hill, V. L. and Nichols, H. R., "Development of Oxidation-Resistant Hafnium Alloys." Final Report. IITRI-B6099-4. 30 September 1970.

55. Brentall, W. D., Klein, M. J., and Metcalf, A. G., "Tungsten Reinforced Oxidation Resistant Columbium Alloys." First Annual Report. Solar RDR 1630-4, January 1970.

56. Douglass, D. L., Oxidation of Metals, 1 (1969) 127.

Table 1. Effect of Low Pressure Pre-oxidation on the 2100°F Nitridation Resistance of Cr-0.22Y

Exposure Time (Hrs.)	Weight Change (mg/cm^2)	
	As-Pickled	Pre-oxidized*
24	12.3	0
96	35.6	5.4

*Pre-oxidized in H_2O atmosphere, 2 hrs. at 1500°F.

Table 2. Pressure Induced Phase Transformations

Compound	Phases	Temp.	Pressure	Ref.
ZrO_2	Meta-stable tetragonal to monoclinic	R.T.	percentage transformed is not a function of pressure above 38 kbar	33
ZrO_2	Cubic stabilized to tetragonal + monoclinic	R.T.		33
PbO_2	I to II		21 kilobar	33
	Tetragonal to tetragonal and orthorhombic (pressure sensitive absorption edge above 20 kbar)	R.T. to 700		
BeO ZnO	cubic - zinc blend - lower temp. hexagon - wurtzite - higher temp. Direct effect of pressure on transition between these two forms is not very likely. Lattice energy difference between wurtizite and zinc blends is only 1%			28
BeO	No transformation	R.T.	45 kbar	28 pg 28
FeO CoO NiO MnO	No phase transitions up to 265 kbar	R.T.	265 kbar	
NiO	Effect of pressure on charge transport (12)			29 pg 56
B_2O_3	20% increase in density-structure not determined			
TiO_2	rutile	20°C	100 kbar	39
	anatase to rutile			38
γ-Fe_2O_3	α-hexagonal-corundum - stable β-cubic-bixbyite - meta-stable γ-tetragonal, 3 spinel blocks - meta-stable ϵ-monoclinic, meta-stable	300°C	33 kbar	28

Table 2. Pressure Induced Phase Transformations (Continued)

Compound	Phases	Temp.	Pressure	Ref.
α-Al_2O_3	no phase transition - compressibility independent of pressure		few hundred kilo bar	28
Cr_2O_3	no phase transition - compressibility is f(P)	R.T.		
α-Fe_2O_3	no phase transition - compressibility increases as a function of pressure			pg 74
V_2O_3	at one atm., temperature dependent monoclinic to corundum at 150°K goes from semi-conducting to metallic behavior. This transition temperature decreased 10°C for 3000 bar pressure increase			28 pg 75
CrO_2	enhanced stability under very high pressure conditions at lower temperatures 275°C - get CrO_3, Cr_2O_3, Cr_6O_{15}, Cr_5O_{12}, and CrO_2 at different pressure temperature conditions.			45
MoC	From Mo & C powders - hex fcc and hexagonal	2000°C	25 kbar	36
MoC	all fcc aging at 1100°C for 5 minutes retained fcc, however, aging at 1600°C caused transformation back to hexagonal MoC and Mo_2C	2000°C	35-90 kbar	

IIA	IVB	VB	VIB	IIIA
Be (hex) (0.31)*				
BeO wurtizite				
Mg (hex) (0.65)				
MgO NaCl				
	(0.90) (+2)	(0.74)(+3)	(0.69) (+3)	
	Ti (hex) (0.64) (+4)	V (bcc)(0.59) (+5)	Cr (bcc)(0.52)(+6)	Al (fcc)(0.50)(+3)
	α TiO cubic	V_2O monoclinic	Cr_2O_3 rhombohedral $D5_1$	αAl_2O_3 rhombehedral C5
	β TiO cubic	VO cubic B1	CrO_2 (unst) rutile	βAl_2O_3 hex: H_{26}
	Ti_2O_3 rhombohedral	V_2O_3 Cr_2O_3	CrO_3 (unst) rhombohedral	$\gamma' Al_2O_3$ defect spinel
	TiO_2 (rutile) - Tetragonal C4	VO_2 tetragonal C4		δAl_2O_3 tetragonal
		V_2O_5 rhombohedral		γAl_2O_3 su
			(0.68)(+4)	χAl_2O_3 γ
Sr fcc (1.13)	Zr (hex) (0.80) (+4)	Nb (bcc) (0.70) (+5)	Mo (bcc) (0.62) (+6)	
SrO NaCl	αZrO_2 Monoclinic	Nb_4O tetra (unst)	MoC_2 monoclinic	
SrO_2 CaC_2	Tetragonal	NbO cubic B1	Mo_4O_{11} rhombohedral	
		NbO_2 tetragonal C4	Mo_9O_{26} monoclinic	
		αNb_2O_5 rhomb (unst)	Mo_8O_{23} monoclinic	
		βNb_2O_5 monoclinic	MoO_3 rhombohedral	
	Hf (hex) (0.81)(+4)	Ta (bcc) (0.73) (+5)	W (bcc) (0.64) (+4) (0.68)(+6)	
	HfO_2 monoclinic	Ta_4O rhomb (unst)	WoO_2 monoclinic	
	HfO_2 tetragonal	Ta_xO - Ta_6O - unst.	W_4O_{11} monoclinic	
		TaO_2 (unst) tetragonal C4	$W_{20}O_{58}$ monoclinic	
		αTa_2O_5 rhombohedral	WO_3 α - triclinic	
		βTa_2O_5 triclinic	β - rhombehedral	

*Numbers in parenthesis denote ionic radius.

Table 3. Structures of Oxides of High Temperature Materials Arranged in a Periodic Fashion

Table 4. Summary of High Pressure Results on Nb_2O_5

Run No.	Time	Temp. °C	Pressure kbar	Film No.	Phases Present[4]*	Color
1	5 min.	1200	78	10,031	(γ+γ'), γ predominates	dark grey
2	15 min.	R.T.	78	10,033	Unidentified	grey
3	15 min.	R.T.	56	10,034	α	white
4	5 min.	1200	56	10,036	(γ'+γ), γ' predominates	dark grey
5	20 min.	R.T.	67	10,037	α+?	grey-white
6	-	-	-	-	-	-
7	5 min.	1200	20	10,038	γ (large crystals)	black
8	1 min.	1200	10	10,039	γ + Form II	black
9	30 min.	800	20	10,041	γ + Trace α	dark grey
10	1 hr.	1200	56	10,042	(γ'+γ), γ' predominates	dark grey
11	16 hr.	400	20	10,043	α + trace of diffuse γ	dark grey
12	30 min.	R.T.	56			
13	30 min.	800	56	10,044	(γ'+γ), γ' predominates	dark grey+black
14	20 hr.	400	56	10,045	(same as Run No. 2)	dark grey+black

(* N. Terao notation)

Table 5. Nomenclatures for Nb_2O_5 Phases

TT	T	B	M	H	N	R	P	ε	I-High	II	Reference
δ(γ')	γ	ζ	β(α')	α	–	–	η	ε	–	–	48
δ	γ	γ'	β	α	–	–	–	–	–	II ($Nb_2O_{4.834}$)	4
–	α	–	β	β	–	–	–	–	–	–	46, 47
diffuse α	α		β	β'	–	–	–	–	–	–	49
–	III	–	II	I	–	–	–	–	I-High at >1300°		50

Table 6. Some Structures of Nb_2O_5
(Notation based on Terao[4] and Brauer[5])

Form	Crystal Structure	a(Å)	b(Å)	c(Å)	β	Density g/cm³
γ (T)	Monoclinic	7.317	15.728	10.749	120°30'	5.815
γ' (B)	Monoclinic	7.348	5.962	13.646	115°30'	
β (M)	Monoclinic	22.10	7.638	19.52	118°15'	
α (H)	Monoclinic	21.20	3.824	19.39	120°10'	4.56
II (-)	Monoclinic (Probable formula $Cb_{12}O_{29}$)	12.03	14.37	10.36	121°10'	

Table 7. Specifications for Grade A Water

Resistivity	$5 \times 10^5 - 10^6$ ohm/cm
pH	(6–7)
Cl-ion conc	< .05 ppm
F-ion conc	< .05 ppm
Total solids	< .05 ppm

Table 8. Results of X-ray Examination of the Films Produced on Ta, Nb, and B-1 Nb Alloy During Exposure in a 350°C Autoclave in Water Doped with Ferric Ions

Sample	Powder Pattern	Diffraction Pattern
Cb	BCC Nb Tapiolite ($FeNb_2O_6$) Nb_2O_5 (several patterns)	Possible BCC α 3.68 β Nb phase Tapiolite oriented Nb
Ta	BCC Ta Ta_2O_5 (several patterns) Many other overlapping line with many possibilities	Strong, sharp tapiolite oriented BCC Ta
B-1	BCC Nb Tapiolite ($FeNb_2O_6$) Nb_2O_5 lines	Very weak tapiolite

Table 9. Summary of the Oxidation Experiments Evaluated, Listing the Material, Environment and Pretreatment

Run	Material	Balance	Environment	Pretreatment	Temperature
9	Ta	Stanton	Air	None	1060°C
13	Ta	Stanton	Air	Autoclave	1060°C
8	Ta	Cahn	O_2 at 20 mm Hg	None	651°C
14	Ta	Cahn	O_2 at 20 mm Hg	Autoclave	651°C
10	Nb	Stanton	Air	None	1060°C
12	Nb	Stanton	Air	Autoclave	1060°C
1	Nb	Cahn	O_2 at 20 mm Hg	None	661°C
7	Nb	Cahn	O_2 at 20 mm Hg	Autoclave	656°C
16	B-1	Stanton	Air	None	1060°C
11	B-1	Stanton	Air	Autoclave	1060°C
18	B-1	Cahn	O_2 at 20 mm Hg	None	653°C
17	B-1	Cahn	O_2 at 20 mm Hg	Autoclave	652°C
19	B-1	Stanton	Air	O_2 at 20 mm Hg	1060°C
20	B-1	Stanton	Air	Autoclave + O_2 at 20 mm Hg	1060°C

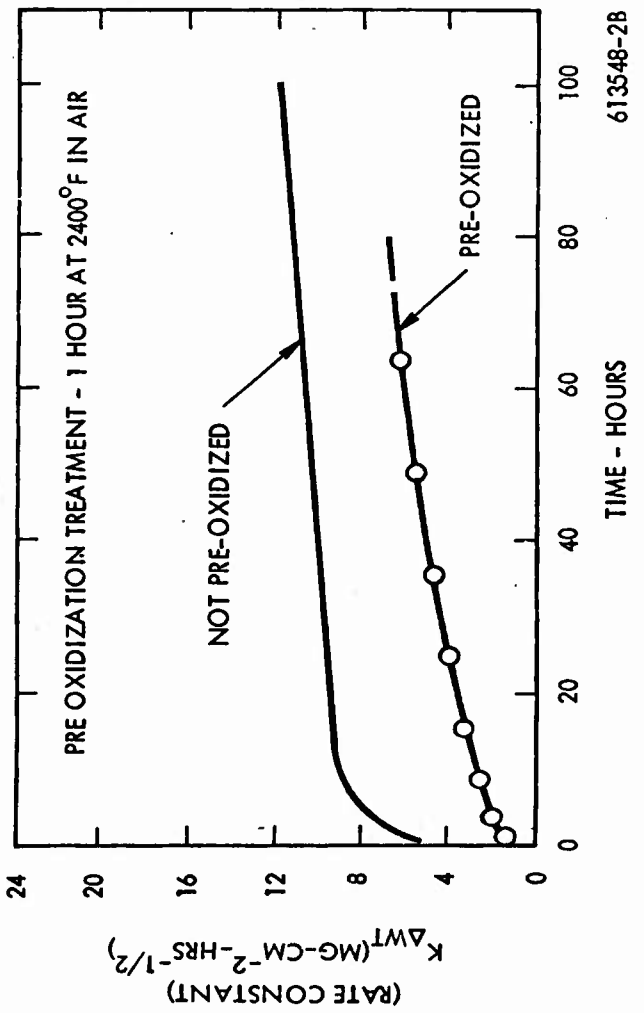

Figure 1. Effect of Pre-oxidation on the 2000°F Oxidation Behavior of a Nb-15Ti-10W-10Ta-2H-3A1 Alloy

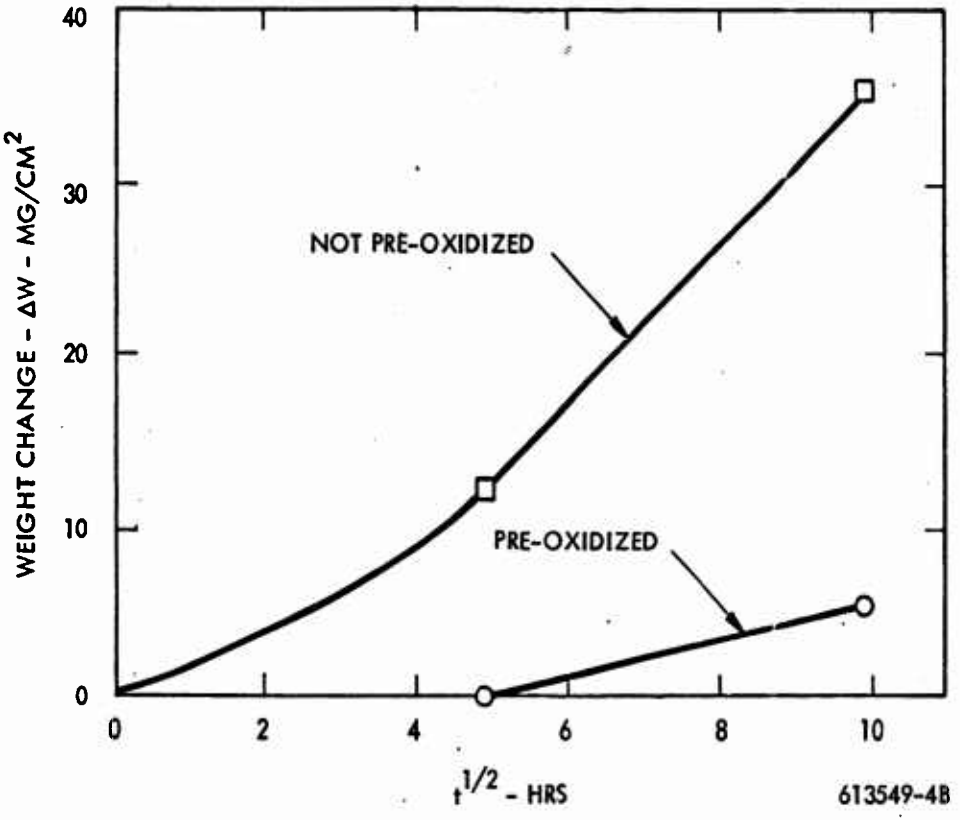

Figure 2. Effect of Pre-oxidation in Low Oxygen Partial Pressure on the 2100°F Nitridation Resistance of Cr-0.224

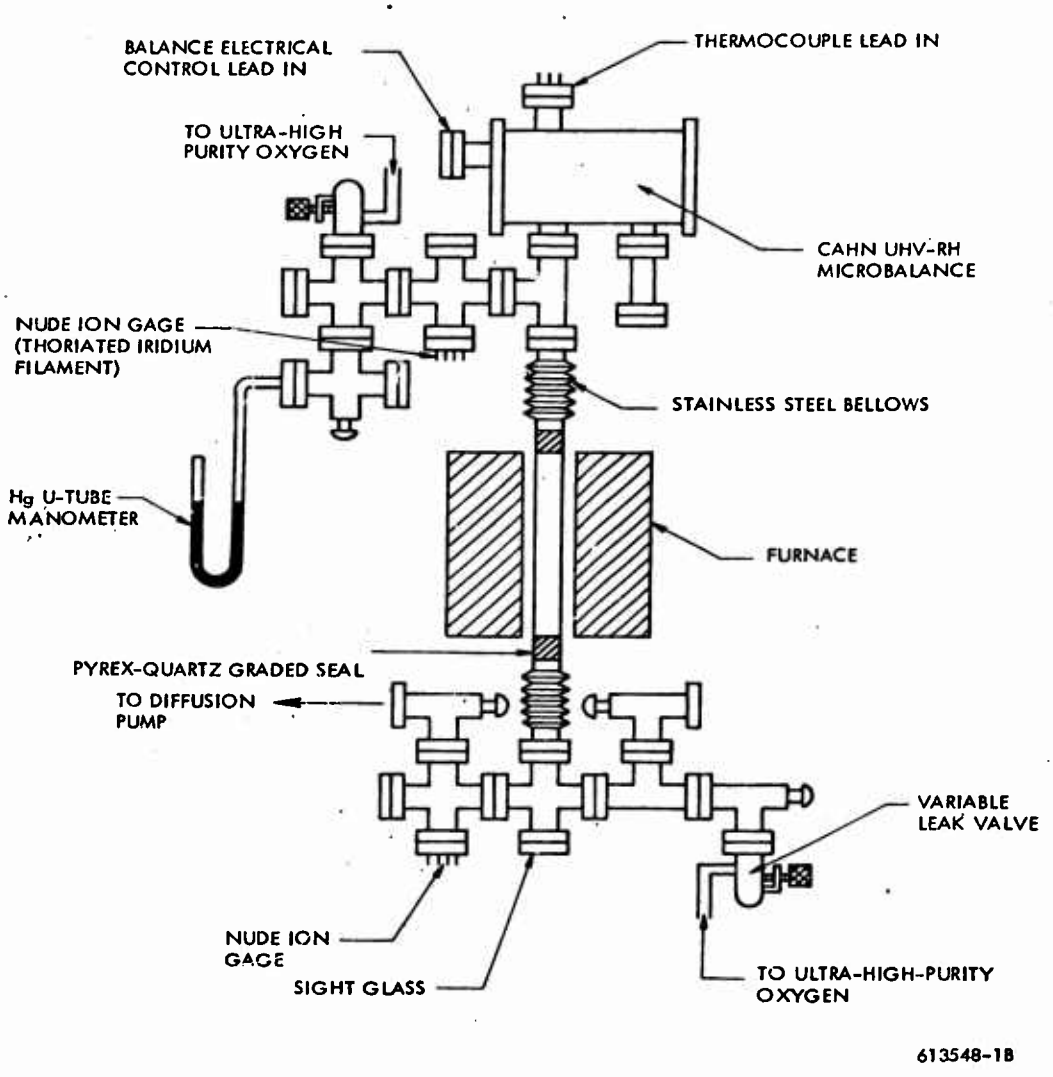

Figure 3. Vacuum Microbalance System Used for Oxidation Rate Studies

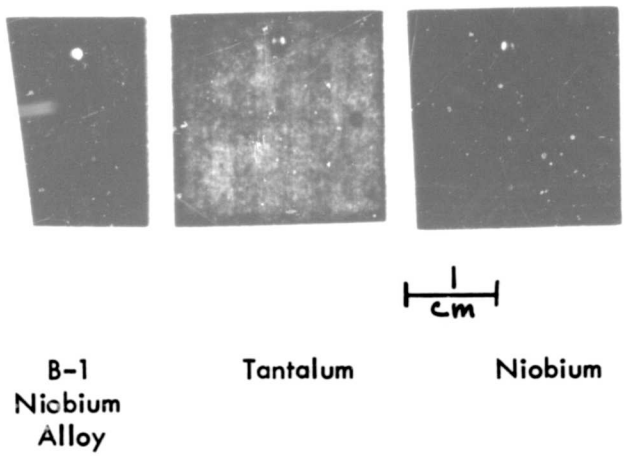

Figure 4. Surface films formed on the Niobium Alloy B-1, Tantalum, and Niobium as a Result of the Autoclave Exposure

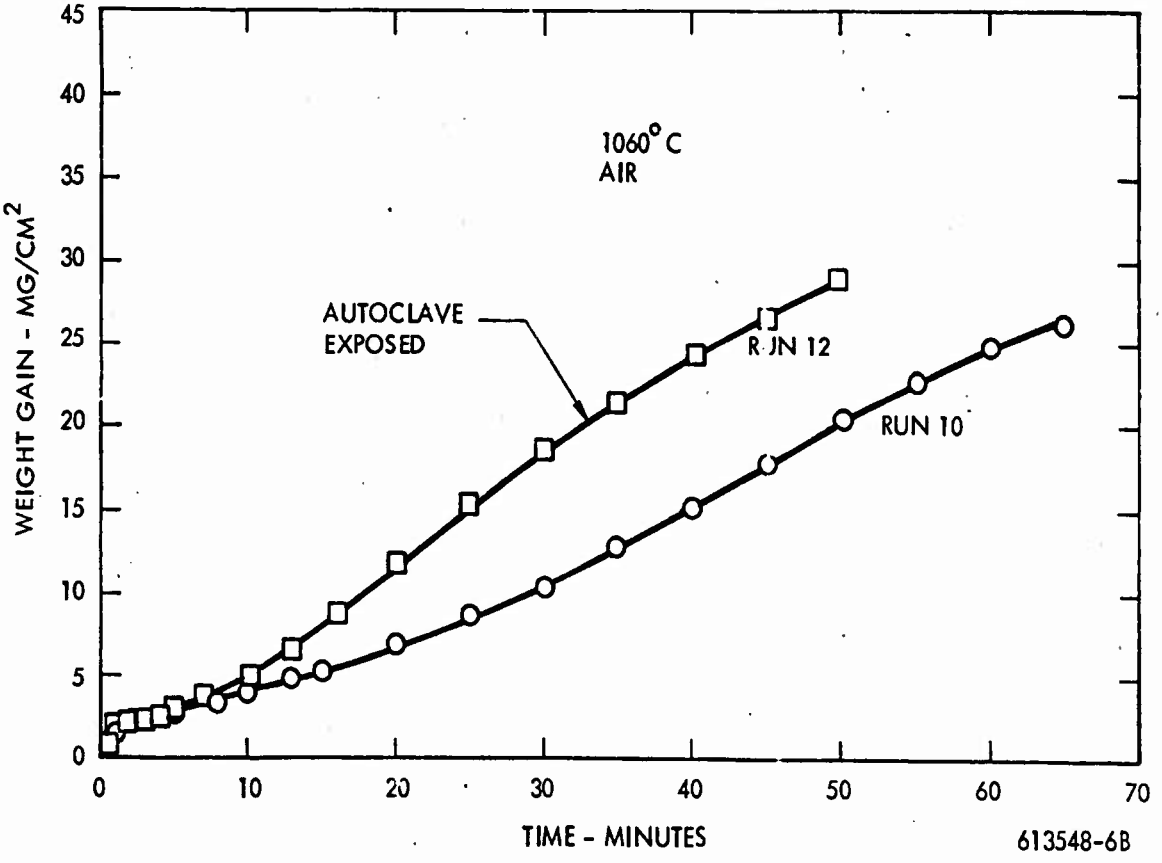

Figure 5. Oxidation Behavior of Niobium in Air at 1060°C with and without the Autoclave Pretreatment

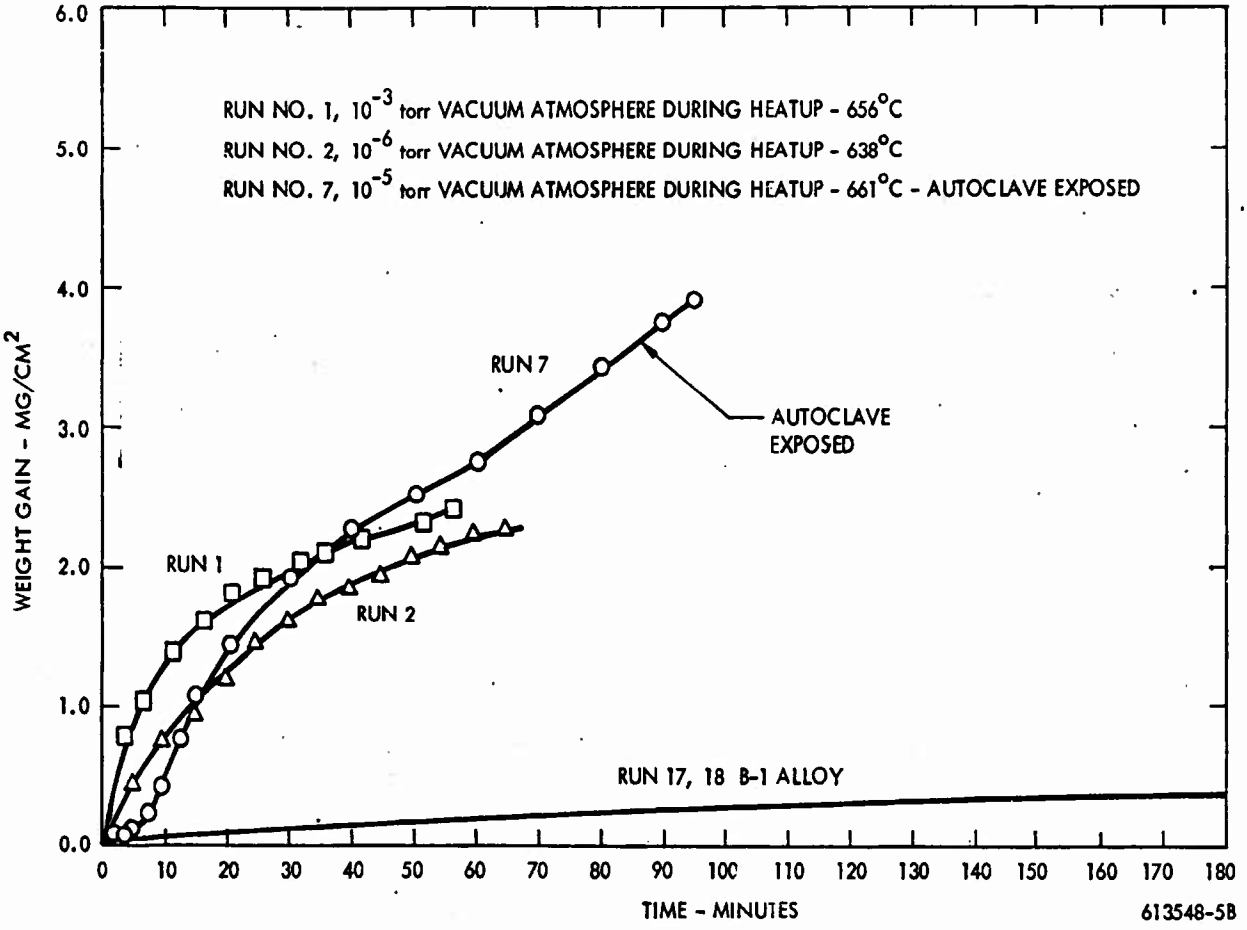

Figure 6. Oxidation Behavior of Nb and the Nb Alloy B-1 in 20 Torr Oxygen at 660°C with and without the Autoclave Pretreatment

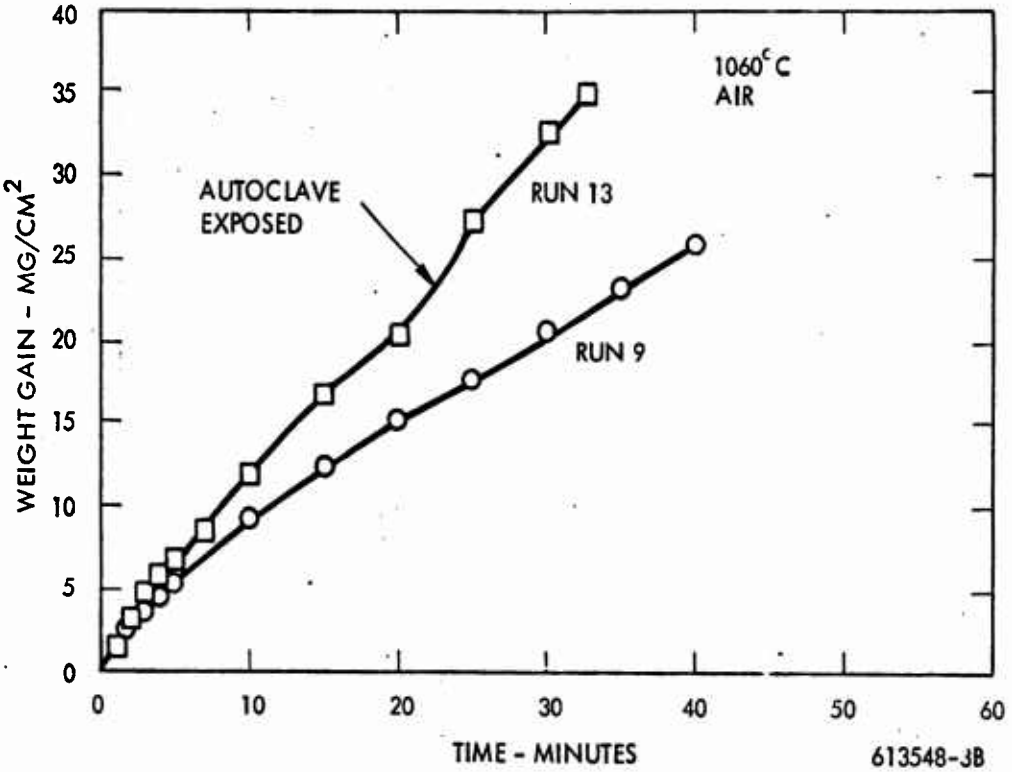

Figure 7. Oxidation Behavior of Ta in Air at 1060°C with and without the Autoclave Pretreatment

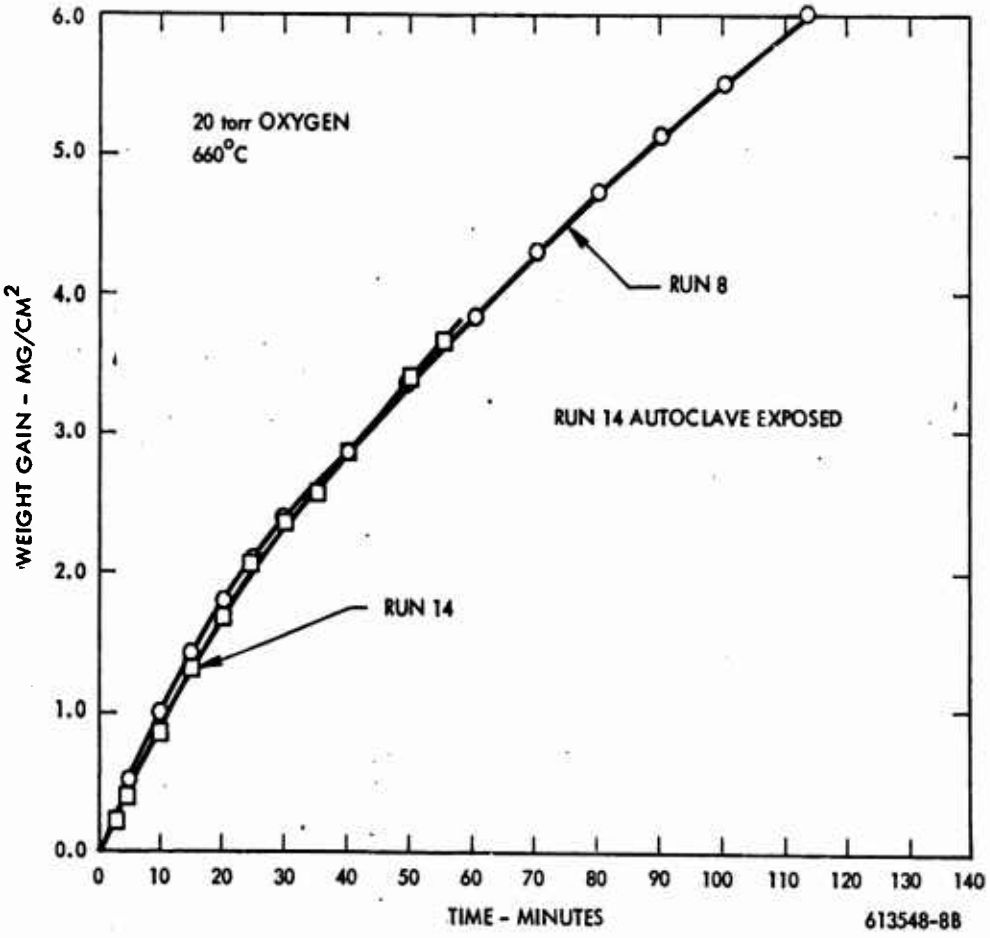

Figure 8. Oxidation Behavior of Ta in 20 Torr Oxygen at 660°C with and without the Autoclave Pretreatment

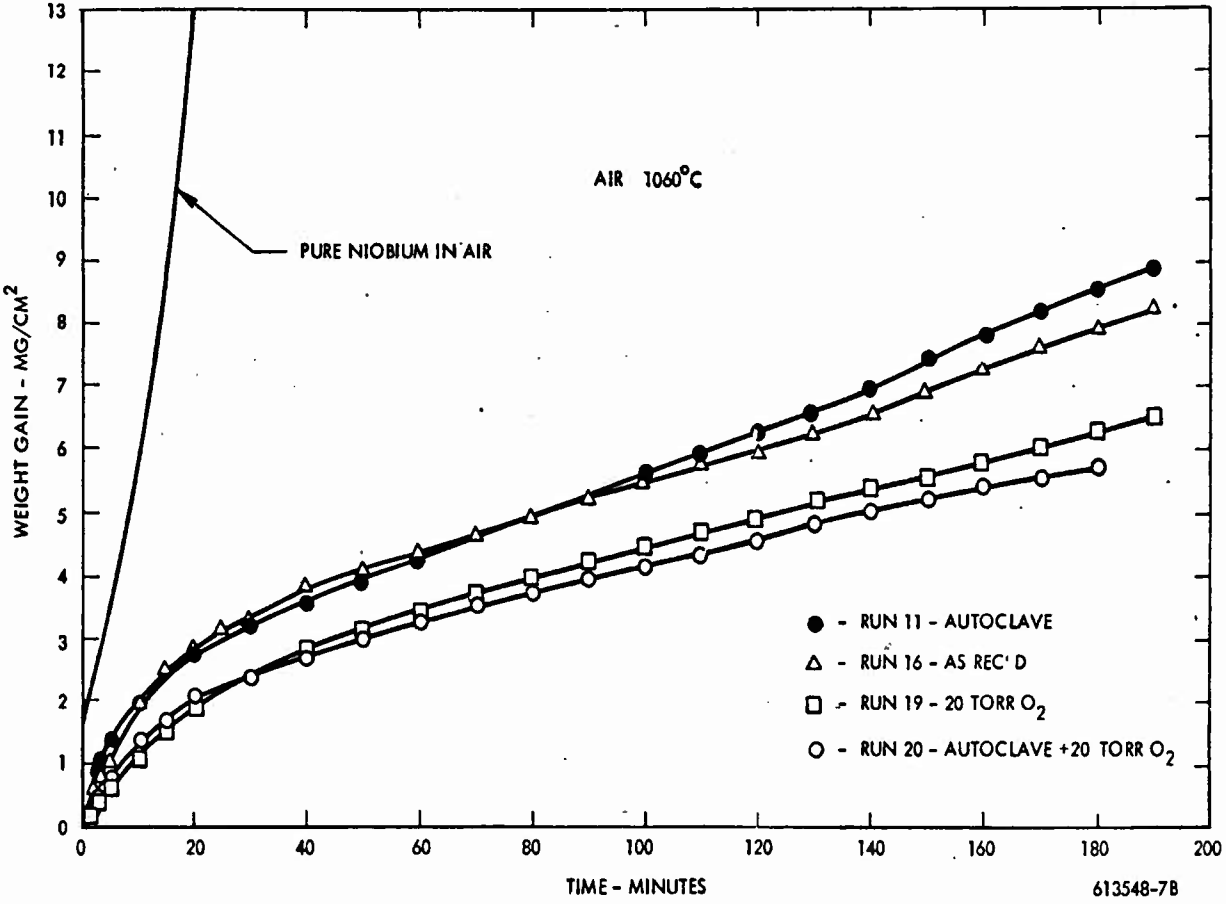

Figure 9. Oxidation Behavior of the B-1 Alloy in Air with and without the Autoclave and/or the 20 Torr Oxygen Pretreatment

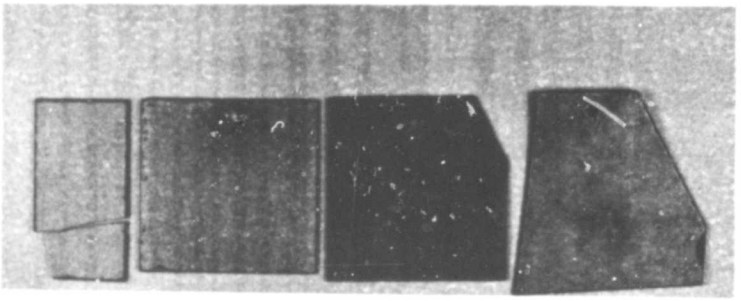

Figure 10. Appearance of B-1 Alloys After Pre-exposures and Air Oxidation. Samples 20 and 11 Pre-exposed in the Autoclave. Surfaces have a Yellow Tint. Surfaces of 16 and 19 are White.

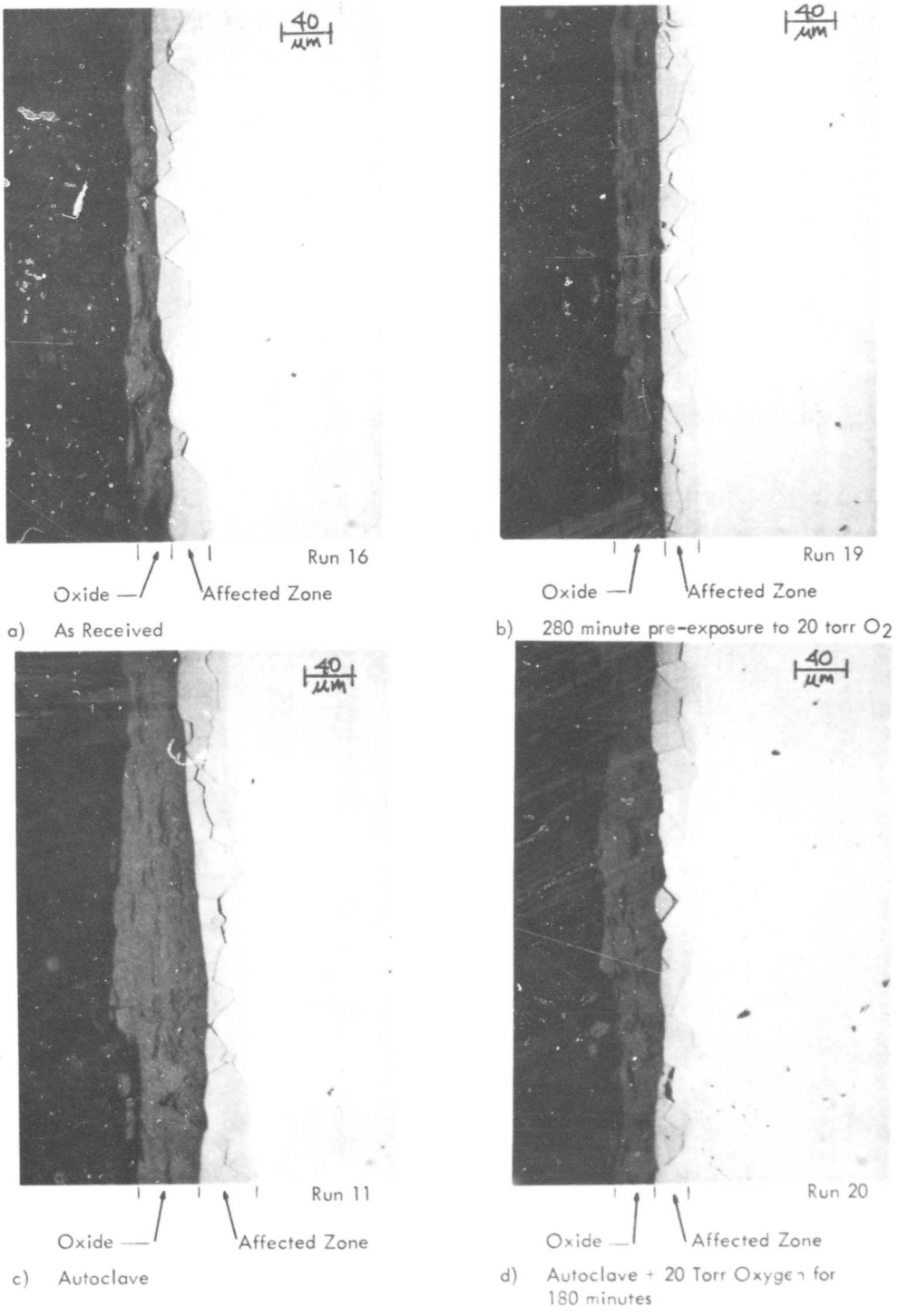

Figure 11. As Polished Photomicrographs of B-1 Alloys. After Air Oxidation Showing the Oxide-Substrate Interface

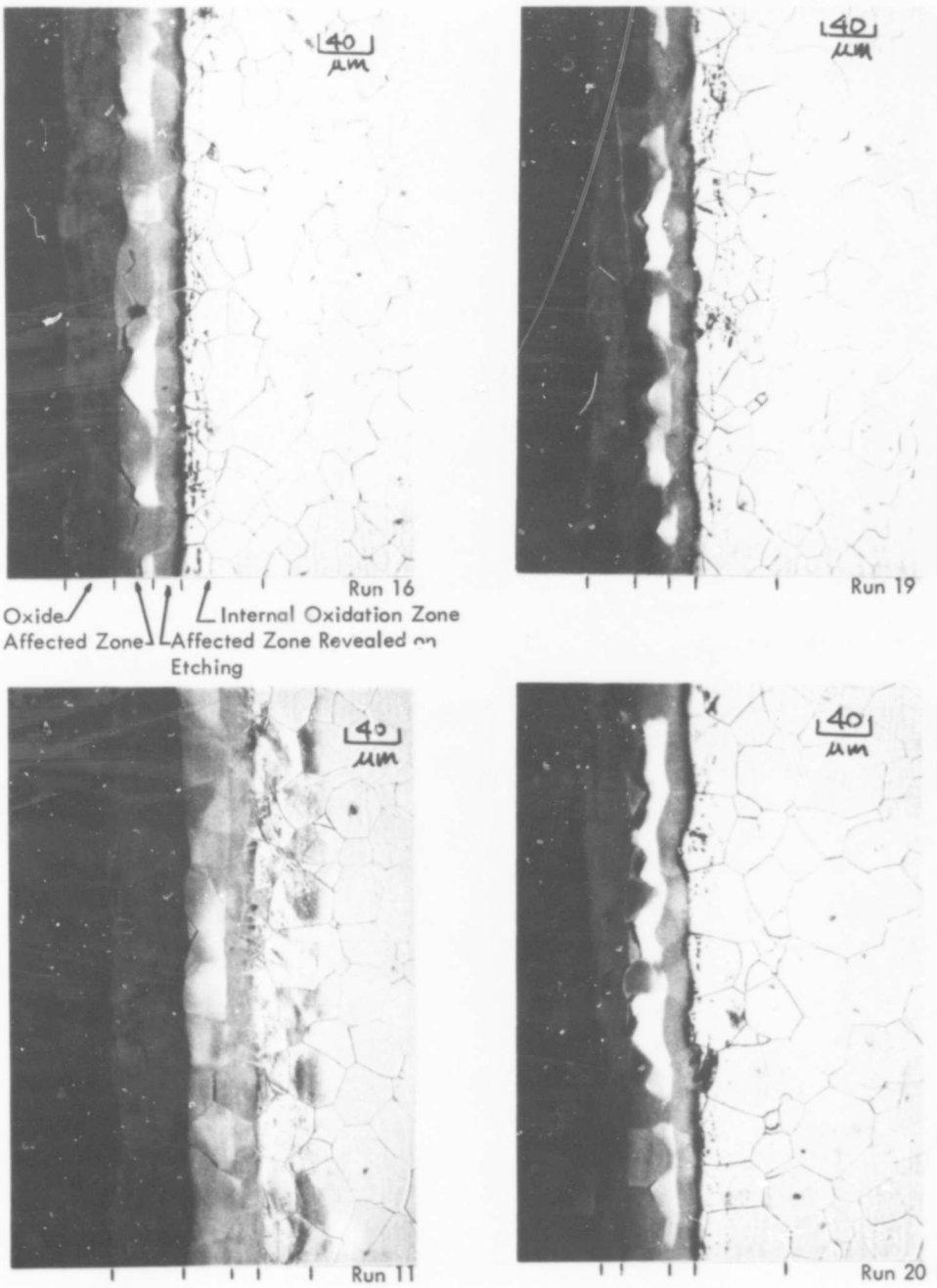

Figure 12. Etched Photomicrographs of B-1 Alloys Showing the Zones Affected by Oxidation

APPENDIX A

Relative Line Intensities and d-Spacing of Oxides Formed During Oxidation Exposures

Table A-1. X-Ray Powder Pattern Results for Samples Exposed in the Autoclave. (350°C Water with Fe^{2})

Tantalum			B-1 Alloy			Niobium		
	I/I0	d-Spacing-Å		I/I0	d-Spacing-Å		I/I0	Å-d-Spacing
1	VW	7.1	1	VW	4.15	1	W	4.15
2	W	5.8	2	VW	3.85	2	W	3.35
3	W	4.15	3	VW	3.60	3	VW	3.15
4	S	3.85	4	VW	3.35	4	VW	2.97
5	W	3.60	5	VW	3.21	5	W	2.58
6	W	3.45	6	VW	3.10	6	VW	2.47
7	W	3.55	7	VW	2.56	7	VW	2.37
8	W	3.24	8	M	2.33	8	S	2.35
9	W	3.10	9	VW	1.74	9	W	1.75
10	W	2.85	10	VW	1.65	10	VW	1.69
11	VW	2.63	11	VW	1.35	11	W	1.66
12	W	2.58				12	VW	1.51
13	W	2.50				13	VW	1.46
14	W	2.43				14	VW	1.41
15	VW	2.37				15	VW	1.37
16	S	2.35				16	M	1.355
17	VW	2.30				17	W	1.175
18	W	2.12						
19	VW	2.00						
20	VW	1.96						
21	W	1.91						
22	VW	1.83						
23	VW	1.79						
24	VW	1.71						

Table A-2. d-Spacings and Relative Intensities for Nb Oxidized in Air

Nb - Run 10			Nb - Run 12			Nb - Run 12 q"		
	I/I_0	d-Spacing-Å		I/I_0	d-Spacing-Å		I/I_0	d-Spacing-Å
1	VW	5.10	1	VW	5.05	1	VW	5.00
2	VW	4.60	2	VW	4.60	2	VW	4.55
3	M	3.73	3	M	3.70	3	S	3.70
4	M	3.62	4	W	3.60	4	W	3.60
5	W	3.50	5	VW	3.52	5	M	3.45
6	M	3.46	6	W	3.45	6	W	3.32
7	VW	3.33	7	VW	3.32	7	VW	3.13
8	VW	3.13	8	W	2.81	8	M	2.81
9	W	2.82	9	W	2.75	9	W	2.75
10	W	2.75	10	VW	2.68	10	W	2.69
11	W	2.69	11	W	2.30	11	W	2.53
12	W	2.53	12	W	2.07	12	VW	2.47
13	VW	2.48	13	W	2.03	13	M	2.30
14	W	2.30	14	M	1.90	14	W	2.07
15	W	2.07	15	VW	1.81	15	W	2.03
16	W	2.03	16	VW	1.78	16	S	1.90
17	M	1.905	17	VW	1.74	17	VW	1.86
18	VW	1.82	18	M	1.68	18	W	1.815
19	VW	1.79	19	VW	1.62	19	W	1.785
20	VW	1.74	20	W	1.58	20	VW	1.76
21	M	1.68	21	W	1.575	21	W	1.735
22	VW	1.62	22	VW	1.55	22	VW	1.70
23	VW	1.585	23	VW	1.52	23	M	1.685
24			24	VW	1.51	24	M	1.675

Table A-3. d-Spacings and Relative Intensities of Nb Oxidized in 20 Torr Oxygen

Nb - Run 1			Nb - Run 2			Nb - Run 7		
	I/I_0	d-Spacing-Å		I/I_0	d-Spacing-Å		I/I_0	d-Spacing-Å
1	S	3.90	1	M	3.95	1	S	3.95
2	S	3.12	2	W	3.20	2	S	3.12
3	M	3.06	3	S	3.12	3	M	3.07
4	VW	2.70	4	W	3.07	4	VW	2.93
5	S	2.44	5	VW	2.71	5	VW	2.70
6	M	2.41	6	VW	2.60	6	M	2.45
7	W	2.11	7	W	2.495	7	W	2.42
8	W	2.01	8	S	2.45	8	VW	2.11
9	M	1.96	9	W	2.43	9	VW	2.01
10	M	1.82	10	W	2.11	10	M	1.96
11	M	1.79	11	W	2.01	11	M	1.825
12	S	1.66	12	M	1.96	12	M	1.79
13	W	1.63	13	VW	1.845	13	VW	1.70
14	W	1.57	14	M	1.82	14	M	1.66
15	VW	1.54	15	M	1.79	15	W	1.63
16	W	1.46	16	M	1.66	16	W	1.57
17	W	1.34	17	W	1.63	17	VW	1.54
18	W	1.32	18	M	1.57	18	VW	1.52
19	VW	1.225	19	VW	1.54	19	W	1.46
20	VW	1.210	20	VW	1.52	20	W	1.34
21	VW	1.195	21	M	1.46	21	W	1.32
22	W	1.145	22	W	1.34	22	W	1.23
23			23	W	1.325	23	VW	1.21
24			24	W	1.230	24	VW	1.195

Table A-4. X-Ray Powder Pattern for Ta Oxidized in Air and 20 Torr Oxygen

Tantalum - Run 9			Tantalum - Run 13			Tantalum - Run 14			Tantalum - Run 8		
	I/I_0	d-Spacing-Å		I/I_0	d-Spacing-Å		I/I_0	d-Spacing-Å		I/I_0	d-Spacing-Å
1	S	3.85	1	S	3.85	1	M	3.85	1	M	3.85
2	S	3.12	2	S	3.12	2	S	3.15	2	S	3.10
3	M	3.08	3	M	3.07	3	S	2.44	3	S	2.43
4	VW	2.70	4	VW	2.70	4	VW	2.00	4	VW	2.00
5	VW	2.63	5	VW	2.61	5	M	1.94	5	M	1.93
6	VW	2.51	6	VW	2.50	6	W	1.83	6	M	1.82
7	S	2.44	7	S	2.44	7	W	1.80	7	W	1.80
8	M	2.40	8	M	2.40	8	VW	1.74	8	S	1.65
9	VW	2.36	9	VW	2.35	9	M	1.65	9	VW	1.57
10	VW	2.09	10	W	2.02	10	W	1.58	10	VW	1.54
11	W	2.02	11	M	1.93	11	W	1.46	11	W	1.46
12	M	1.93	12	M	1.82	12	VW	1.40	12	W	1.44
13	M	1.825	13	M	1.79	13	W	1.33	13	VW	1.40
14	M	1.795	14	W	1.76	14	W	1.32	14	W	1.33
15	W	1.76	15	S	1.65	15	VW	1.29	15	W	1.32
16	S	1.65	16	VW	1.62	16	VW	1.22	16	VW	1.295
17	VW	1.625	17	VW	1.60	17	W	1.195	17	VW	1.22
18	VW	1.60	18	W	1.57	18	VW	1.145	18	W	1.195
19	W	1.57	19	W	1.55	19					
20	W	1.55	20	VW	1.49	20					
21	VW	1.495	21	VW	1.48	21					
22	VW	1.48	22	W	1.455	22					
23	W	1.46	23	W	1.435	23					
24	W	1.435	24	W	1.400	24					

Table A-5. d-Spacings and Relative Intensities from X-Ray Powder Patterns for B-1 Alloys Oxidized in Air

B-1 Alloy - Run 19			B-1 Alloy - Run 20			B-1 Alloy - Run 11			B-1 Alloy - Run 16		
	I/I_0	d-Spacing-Å		I/I_0	d-Spacing-Å		I/I_0	d-Spacing-Å		I/I_0	d-Spacing-Å
1	VW	5.05	1	VW	5.10	1	VW	5.10	1	VW	5.05
2	VW	4.75	2	VW	4.80	2	VW	4.80	2	VW	4.75
3	S	3.72	3	S	3.75	3	S	3.72	3	S	3.73
4	M	3.55	4	M	3.55	4	M	3.55	4	M	3.52
5	M	3.40	5	M	3.41	5	M	3.40	5	M	3.40
6	M	3.24	6	M	3.25	6	W	3.24	6	M	3.25
7	M	2.76	7	M	2.77	7	M	2.77	7	M	2.77
8	VW	2.69	8	VW	2.70	8	VW	2.68	8	VW	2.70
9	W	2.48	9	VW	2.52	9	W	2.49	9	W	2.48
10	M	2.30	10	W	2.49	10	M	2.30	10	W	2.34
11	VW	2.19	11	M	2.30	11	VW	2.19	11	M	2.30
12	M	2.04	12	VW	2.19	12	M	2.04	12	VW	2.19
13	M	1.90	13	S	2.04	13	M	1.905	13	M	2.04
14	W	1.77	14	S	1.90	14	W	1.77	14	M	1.90
15	W	1.69	15	W	1.77	15	W	1.69	15	W	1.77
16	M	1.67	16	W	1.69	16	W	1.67	16	M	1.69
17	VW	1.625	17	M	1.67	17	VW	1.62	17	M	1.67
18	W	1.565	18	VW	1.63	18	W	1.57	18	VW	1.62
19	VW	1.52	19	W	1.57	19	VW	1.45	19	W	1.57
20	VW	1.48	20	VW	1.485	20	W	1.395	20	VW	1.45
21	VW	1.455	21	W	1.45	21	VW	1.365	21	M	1.395
22	VW	1.445	22	M	1.395	22	VW	1.35	22	VW	1.36
23	W	1.390	23	VW	1.365	23	VW	1.30	23	VW	1.35
24	VW	1.360	24	VW	1.350	24	VW	1.265	24	VW	1.34

Table A-6. d-Spacings and Relative Intensities for X-Ray Diffraction Plots for B-1 Alloys Oxidized in Air

B-1 Alloy - Run 11			B-1 Alloy - Run 16			B-1 Alloy - Run 19			B-1 Alloy - Run 20		
	I/I_0	d-Spacing-Å		I/I_0	d-Spacing-Å		I/I_0	d-Spacing-Å		I/I_0	d-Spacing-Å
1	17	5.13	1	22	5.13	1	21	5.07	1	21	5.13
2	12	4.80	2	10	4.86	2	21	4.88	2	14	4.86
3	100	3.74	3	2	4.58	3	100	3.74	3	11	4.73
4	31	3.54	4	100	3.74	4	61	3.54	4	100	3.74
5	46	3.43	5	46	3.54	5	57	3.43	5	50	3.54
6	15	3.35	6	37	3.50	6	14	3.35	6	50	3.50
7	52	3.20	7	46	3.43	7	32	3.20	7	64	3.43
8	58	2.78	8	12	3.35	8	68	2.78	8	14	3.35
9	15	2.696	9	41	3.20	9	14	2.696	9	36	3.20
10	10	2.543	10	58	2.78	10	11	2.564	10	68	2.777
11	21	2.496	11	12	2.735	11	18	2.529	11	18	2.696
12	21	2.310	12	12	2.696	12	54	2.496	12	64	2.496
13	4	2.200	13	10	2.543	13	32	2.310	13	43	2.310
14	27	2.054	14	27	2.496	14	11	2.197	14	14	2.197
15	35	1.907	15	17	2.310	15	50	2.054	15	46	2.054
16	10	1.781	16	5	2.197	16	46	1.907	16	36	1.907
17	8	1.768	17	37	2.054	17	14	1.775	17	11	1.775
18	19	1.690	18	39	1.907	18	7	1.743	18	7	1.716
19	27	1.670	19	10	1.781	19	11	1.716	19	18	1.698
20	4	1.634	20	27	1.691	20	43	1.690	20	36	1.676
21	15	1.570	21	34	1.680	21	46	1.676	21	18	1.570
22	4	1.542	22	12	1.570	22	25	1.570	22	11	1.486
23	4	1.524	23	2	1.455	23	25	1.397	23	14	1.397
24	12	1.397	24	17	1.397						

APPENDIX B

X-Ray Powder Patterns of Oxides Formed During Oxidation Exposures

Tantalum

Niobium

Niobium Alloy B-1

Figure B-1. X-Ray Powder Patterns Taken from the Scraped Surface of Ta, Nb, and B-1 Exposed in the Autoclave

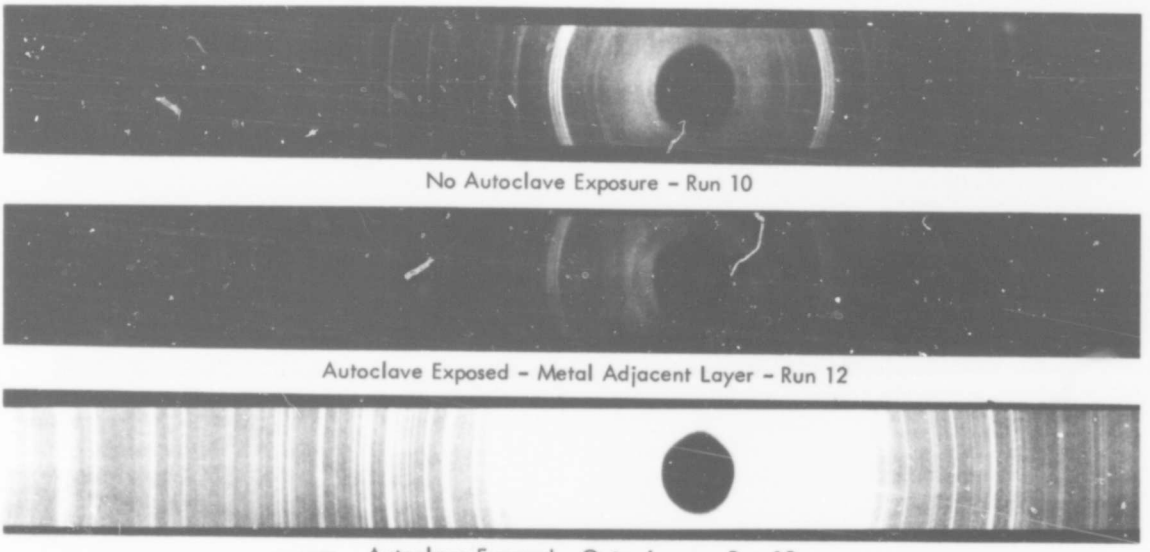

No Autoclave Exposure - Run 10

Autoclave Exposed - Metal Adjacent Layer - Run 12

Autoclave Exposed - Outer Layer - Run 12

Figure B-2. X-Ray Powder Patterns for Nb Oxides Grown in Air at 1060°C

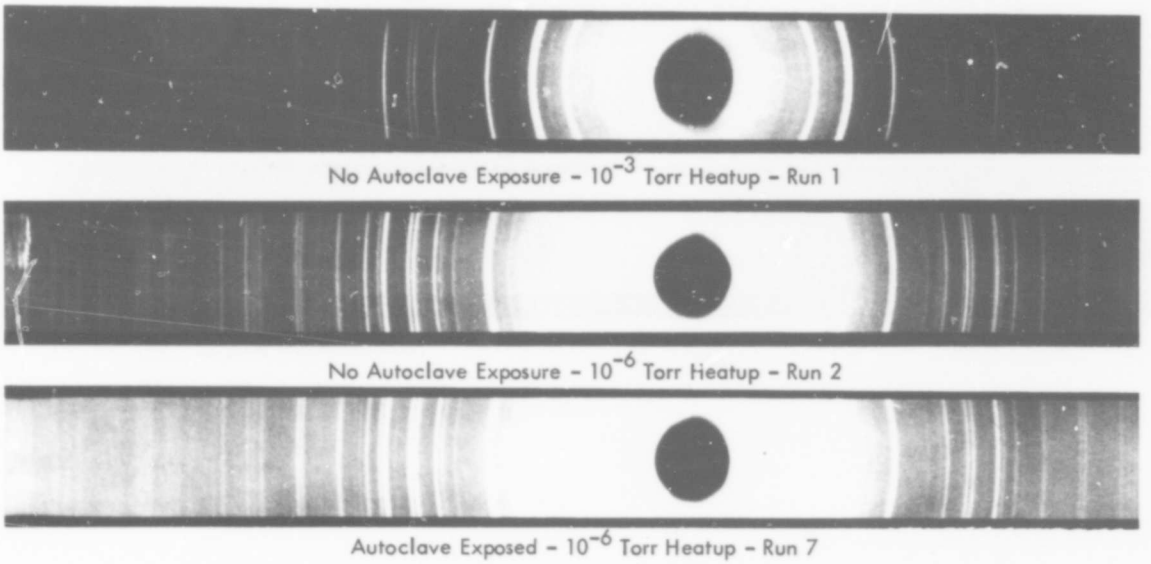

No Autoclave Exposure - 10^{-3} Torr Heatup - Run 1

No Autoclave Exposure - 10^{-6} Torr Heatup - Run 2

Autoclave Exposed - 10^{-6} Torr Heatup - Run 7

Figure B-3. X-Ray Powder Patterns for Nb Oxides Grown in 20 Torr Oxygen at 660°C

No Autoclave Exposure - Run 9

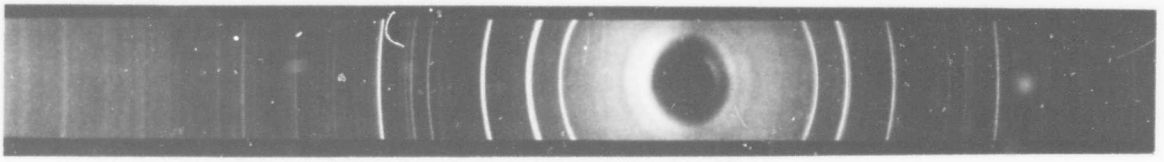

Autoclave Exposure - Run 13

NOT REPRODUCIBLE

a) X-Ray Powder Patterns for Ta Oxides Grown in Air at 1060°C

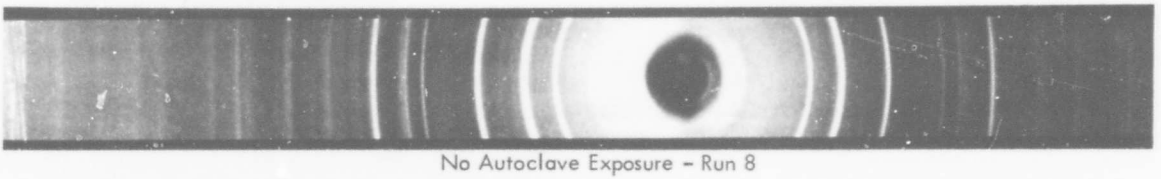

No Autoclave Exposure - Run 8

Autoclave Exposure - Run 14

Figure B-4. b) X-Ray Powder Patterns for Ta Oxides Grown in 20 Torr Oxygen

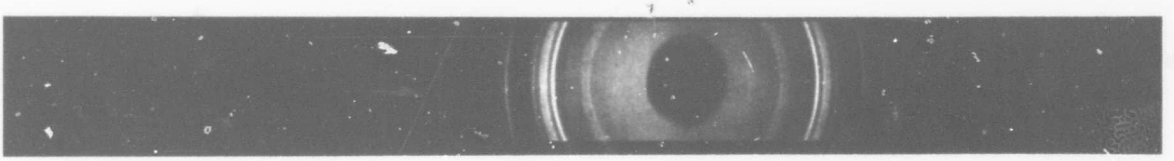

Autoclave Exposure - Run 11

As Received - Run 16

a) X-Ray Powder Patterns of Oxides Formed on B-1 in Air at 1060°C

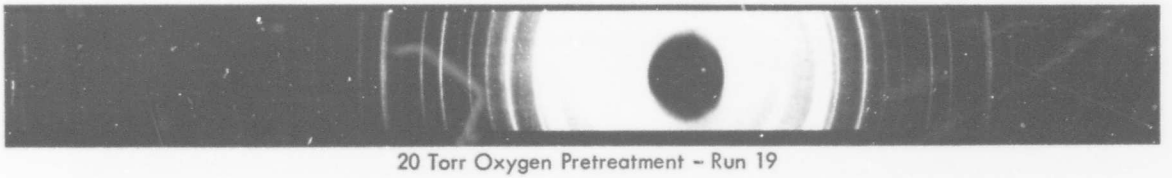

20 Torr Oxygen Pretreatment - Run 19

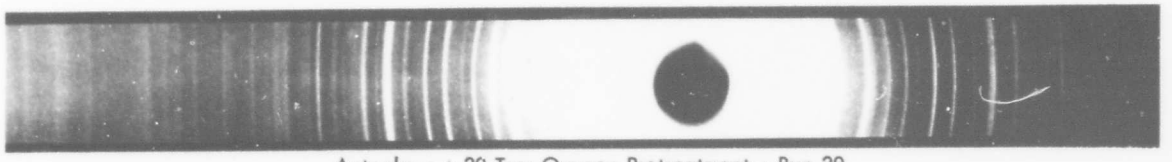

Autoclave + 20 Torr Oxygen Pretreatment - Run 20

Figure B-5. b) X-Ray Powder Patterns of Oxides Formed on B-1 in Air at 1060°C